Observations of Chain Aggregates in Florida Cirrus Cloud Anvils on 3 August 2019 during CapeEx19

Christian Nairy

Master’s Thesis Defense

University of North Dakota

14 July 2022

Committee Members:
Dr. David Delene*, UND
Prof. Michael Poellot, UND
Dr. Jerome Schmidt, NRL-MRY
Dr. Paul Harasti, NRL-MRY

* - Committee Chair

Objective

Is chain aggregation occurring in the cirrus cloud anvil region of Florida thunderstorms on 3 August 2019?

PHIPS image of a chain aggregate

Motivation for Research

- The chain aggregation process is still not well understood.
  - Where/How?
  - Inconsistencies between cloud chamber experiments and aircraft observations.
  - Lack of representation in atmospheric cloud models.

- Cirrus Clouds are Important.

- Influence on radiative transfer properties of cirrus clouds (Liou 1973; Stephens *et al*. 1990; Baran 2009).

UND UNIVERSITY OF NORTH DAKOTA

Motivation for Research

- Chain aggregates may alter supersonic projectile trajectories (Lin and Thyson 1977; Meng and Ludema 1995; Barnes Jr. 1982).

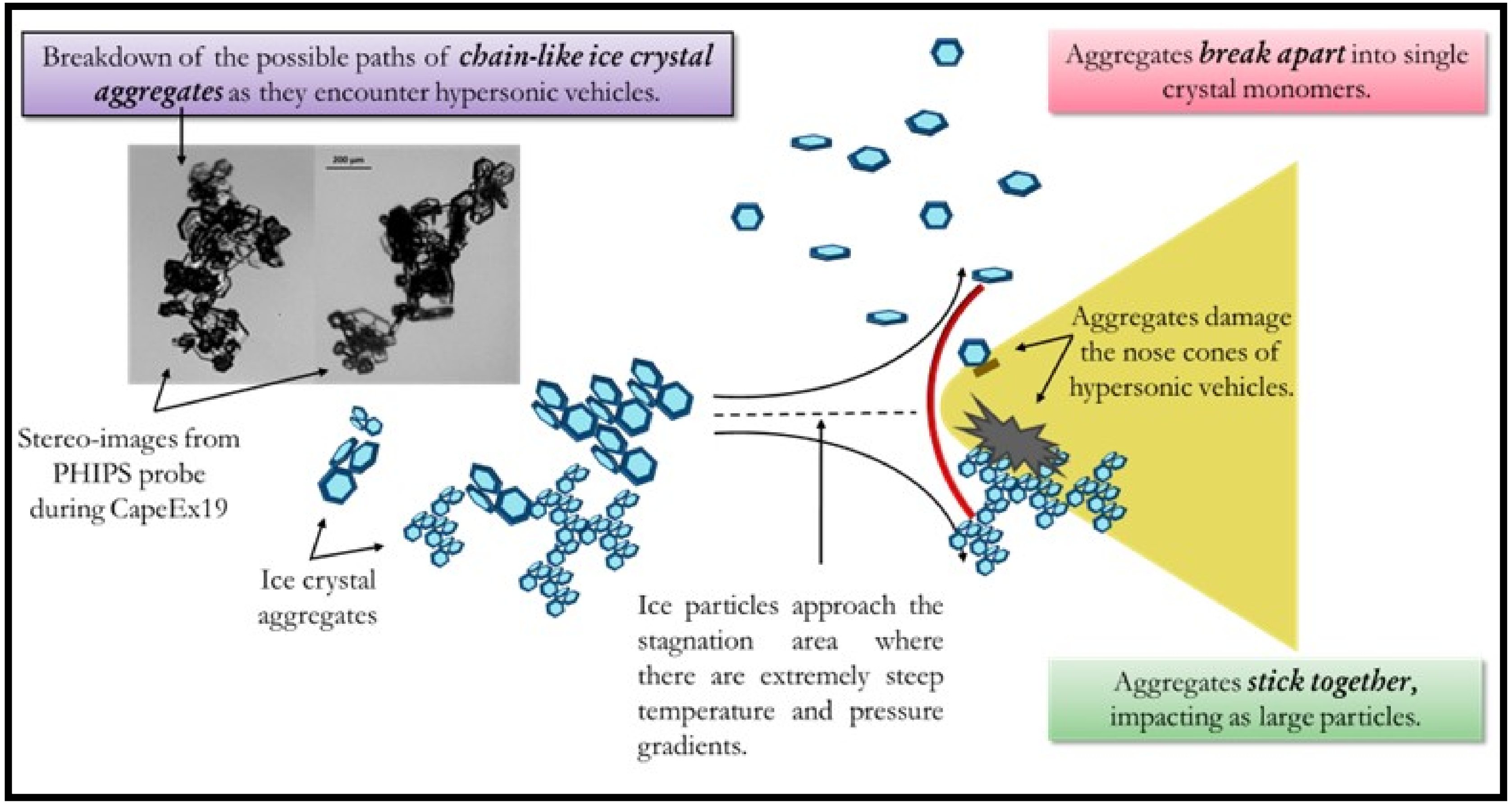

Image obtained courtesy of Hallie Chelmo from the University of North Dakota’s Mechanical Engineering Department.

Cloud Chamber Experiments

- Several cloud chamber experiments have investigated the chain aggregation process.

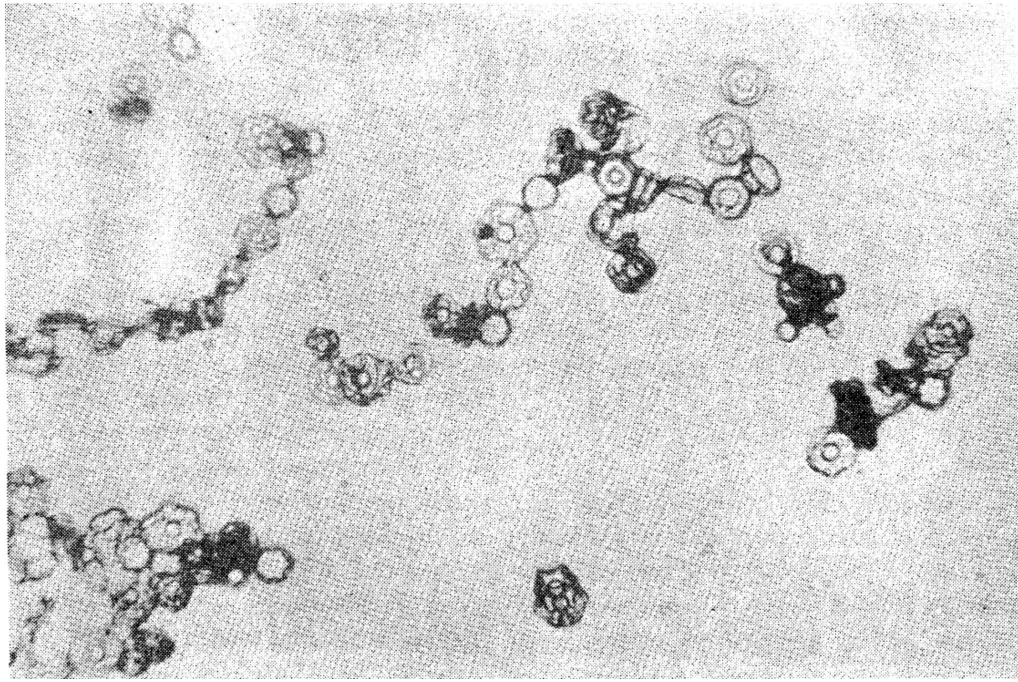

Adapted from Saunders and Wahab, 1975.

- Chain Aggregates Where Generated:
  - In high Electric Fields (Minimum Threshold: 60 kV m^{-1})
  - In Temperatures Between -5 and -37 °C
  - Ice Crystal Concentrations Between 3 and 4 $\times$ 10^6 m^{-3}
  - Ice Crystals Sizes Between 30 to 50 μm

- Aggregation increases 30% in electric fields (10^2 kV m^{-1}) at T = -8 °C (Maximum effect).
- Aggregation found to be temperature dependent with electric fields.

Previous Aircraft Observations

- Chain Aggregates of **Pristine** Ice Crystals Observed
  - Continental convection (with some maritime influence) in the tropics and sub-tropics.
  - -25 to -65 °C

- Chain Aggregates of **Frozen Droplets** Observed
  - Continental Convection in the Midlatitudes.
  - -13 to -60 °C

- Chain aggregates observed near updraft region of a Florida thunderstorm
  - -8 °C
  - Some Riming Present

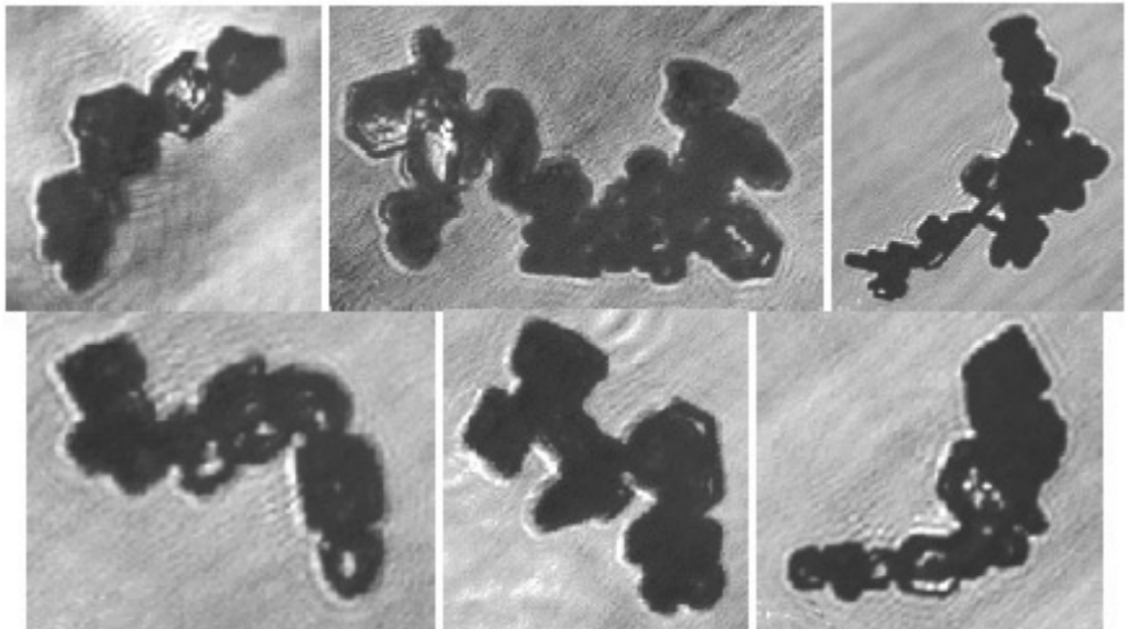

Chain aggregates comprised of ice crystals imaged during the EMERALD-II experiment. Adapted from Connolly *et al.* 2005.

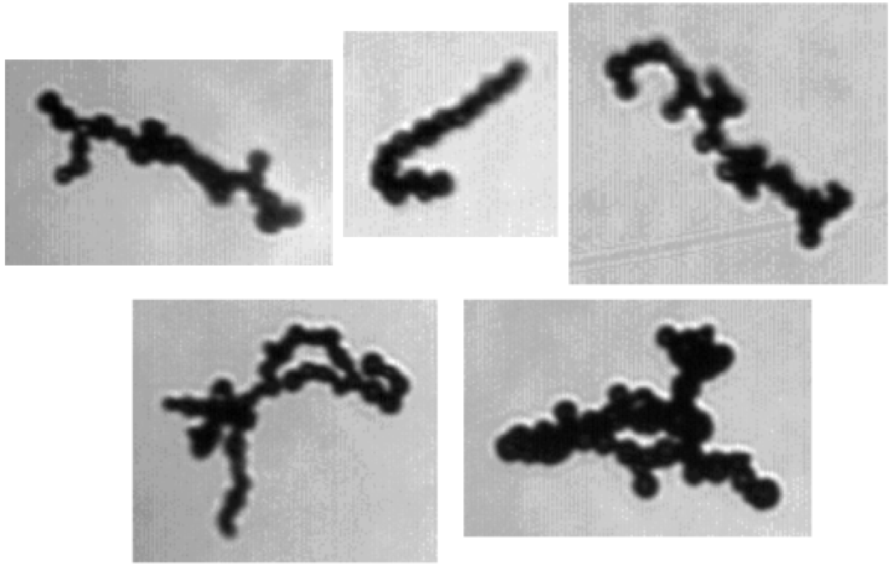

Chain aggregates comprised of frozen droplets observed in mid-latitude cirrus anvil clouds. Adapted from Stith *et al.* 2014.

CAPE Experiment 2015 (CAPE2015)

- Performed near Cape Canaveral, Florida, from 28 July to 11 August 2015.
- Airborne sampling of Florida convection-induced, cirrus anvils.
- Chain-like Aggregates Observed.
- Chains appear to have plate-like elements.
  - Altitudes ~11 km and Temperatures of ~ -43 °C.
- Poor Resolution and Image Quality of the 2D-S
  - Difficult visualizing each chain aggregate element and discerning the exact crystal habits.

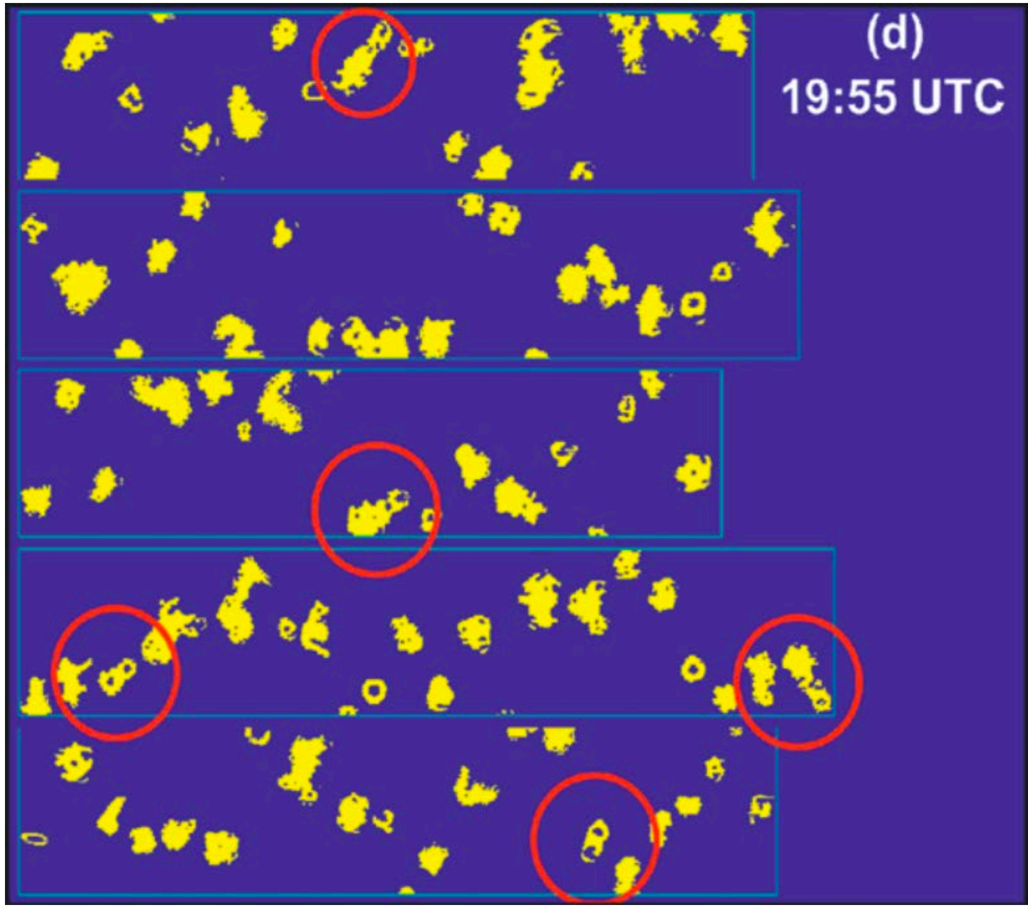

Adapted from Schmidt *et al*. 2019.

CAPE Experiment 2019 (CapeEx19)

- Near Cape Canaveral, Florida, from 22 July to 3 August 2019

- Sampled convection-induced, cirrus cloud anvils

- Concurrent measurements between in-situ (aircraft) and remote-sensed platforms (radar).

- Goals:
  1. Investigate the presence of chain aggregates/chain aggregation
  2. Improve radar interpretation
  3. Improve cirrus cloud modeling

The North Dakota Citation II Research Aircraft at the Space Coast Regional Airport in Titusville, Florida.

Instrumentation

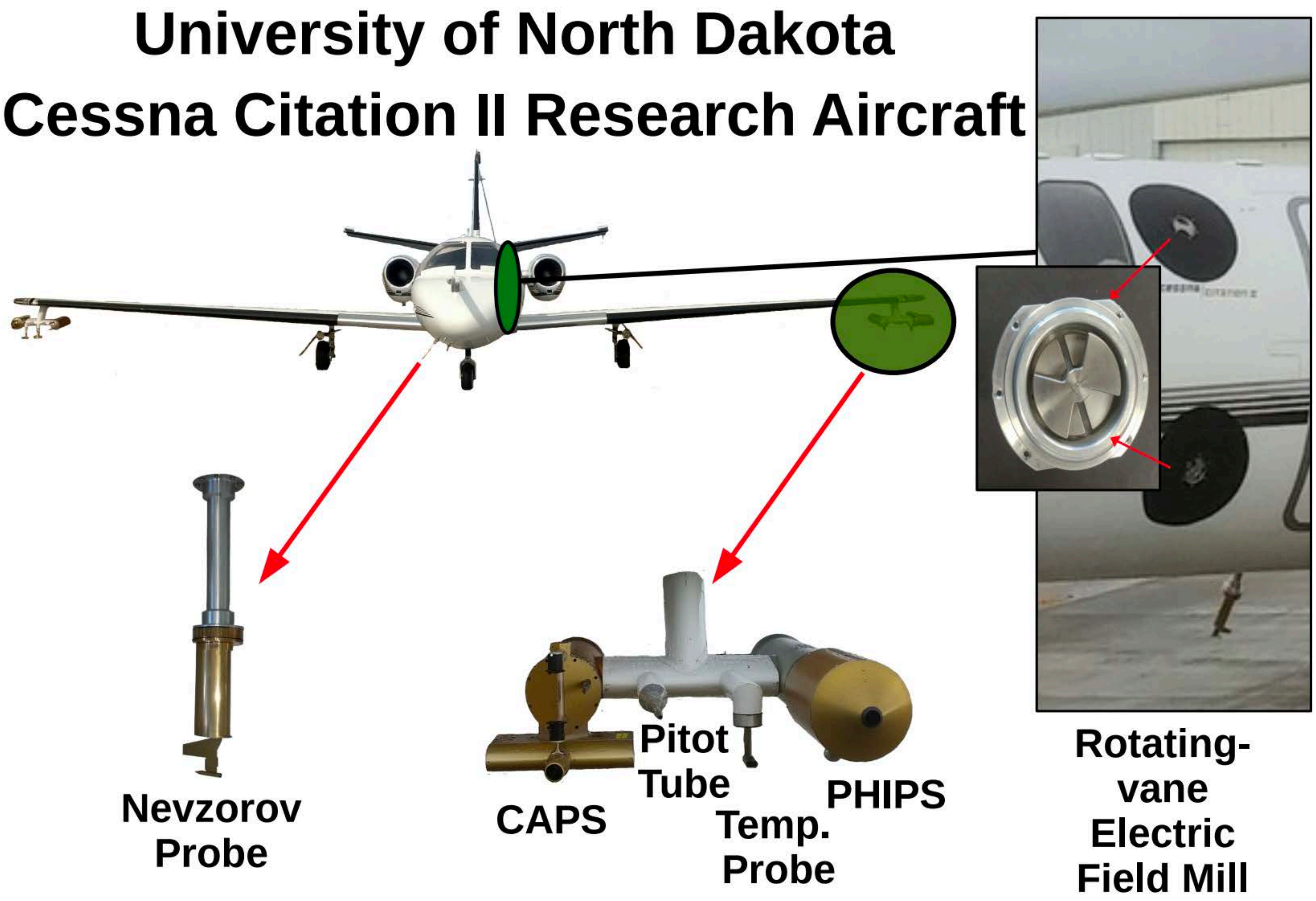

Particle Habit Imaging and Polar Scattering (PHIPS) Probe

- Provide clarity into the link between the microphysical characteristics of individual ice particles and their respected angular light scattering function (Schnaiter *et al.* 2018).

- Hybrid between the airborne polar nephelometer (PN) and the Cloud Particle Imager (CPI) probe.

- High definition, stereographic images of the same cloud particle
  - two viewing angles separated by an angular distance of 120 °

- Optical magnifications from low (1.4 ×) to high (9.0 ×) with an optical resolution range from 7.2 to 2.35 μm, respectively.

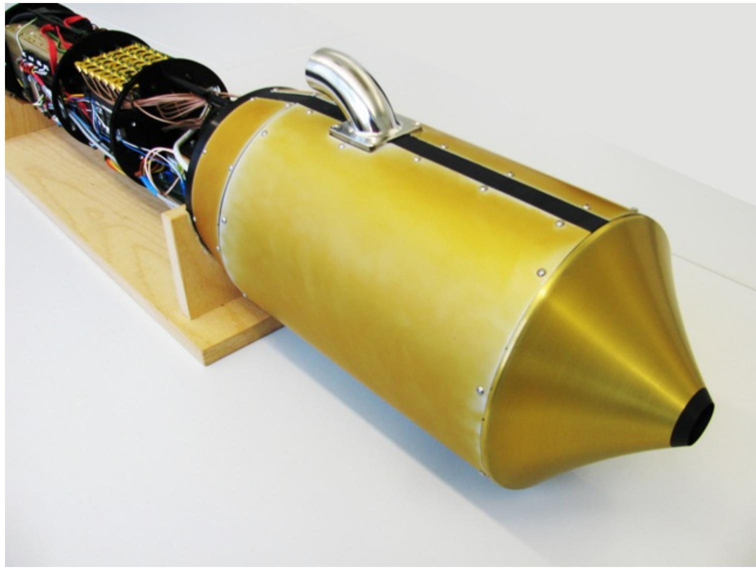

Image of the PHIPS (KIT 2022).

UND UNIVERSITY OF NORTH DAKOTA

Cloud Imaging Probe (CIP)

- One of the instruments associated with the Cloud, Aerosol, and Precipitation Spectrometer (CAPS).
- Provides shadow images of cloud particles.
- Particle size range of 12.5 µm – 1.55 mm (resolution of 25 µm) with a sample area of 10 cm x 1.55 mm.
- Processing of particle data obtained by the CIP performed using the System for Optical Array Probe Data Analysis Version 2 (SODA2) software package (Bansemer 2013).

Image of the CAPS probe.

UNIVERSITY OF NORTH DAKOTA

Rotating-vane Electric Field Mills

- Total of 6 electric field mills on the aircraft.
  - Provided by the University of Alabama in Huntsville (UAH)

- The electric field values are calculated as a result of the time-varying charge induced on the sensing plates by the ambient electric field (Bateman *et al.* 2007).

- The reference coordinate system:

– x-axis (E_x) along the fuselage of the aircraft (roll axis), where E_x is positive in the direction of flight

– y-axis (E_y) being along the wings of the aircraft (pitch axis), where E_y is positive out the left wing (port)

– z-axis (E_z) being perpendicular to the fuselage and the wings of the aircraft, where during level flight, E_z is positive up.

Image of port side electric field mills.

Remote-sensed Platforms and Datasets

- Melbourne, Florida National Weather Service (NWS) Next-Generation Radar (NEXRAD) WSR-88D (KMLB)
- Cloud and Precipitation Radar with Discrete Hydrometeor Detection (CPR-HD)
- National Lightning Detection Network (NLDN)
- Kennedy Space Center’s (KSC) Lightning Mapping Array (LMA)

Image of the CRP-HD at the KSC

Methods

Case Study for the 3 August 2019 Flight Day

- Classify Chain Aggregates
- Analyze the distribution of chain aggregates in the cirrus anvil
- Chain Aggregate Concentrations
  - Calculate a relative chain aggregate concentrations
- Electric Field Analysis
- Put the in-situ microphysical and electrical observations into context by using the remote-sensed datasets.

Chain Aggregate Definition

Chain Aggregates are **defined** by:

- Three or more discernable particles oriented in a quasi-linear fashion.
- Particles joined together by small joints.
- Links of particles that are unusually elongated.

Confidence is determined by the classifier:

- Low confidence (1): One of the three definitions observed.
- Moderate confidence (2): Two of the three definitions observed.
- High confidence (3): All three definitions observed.

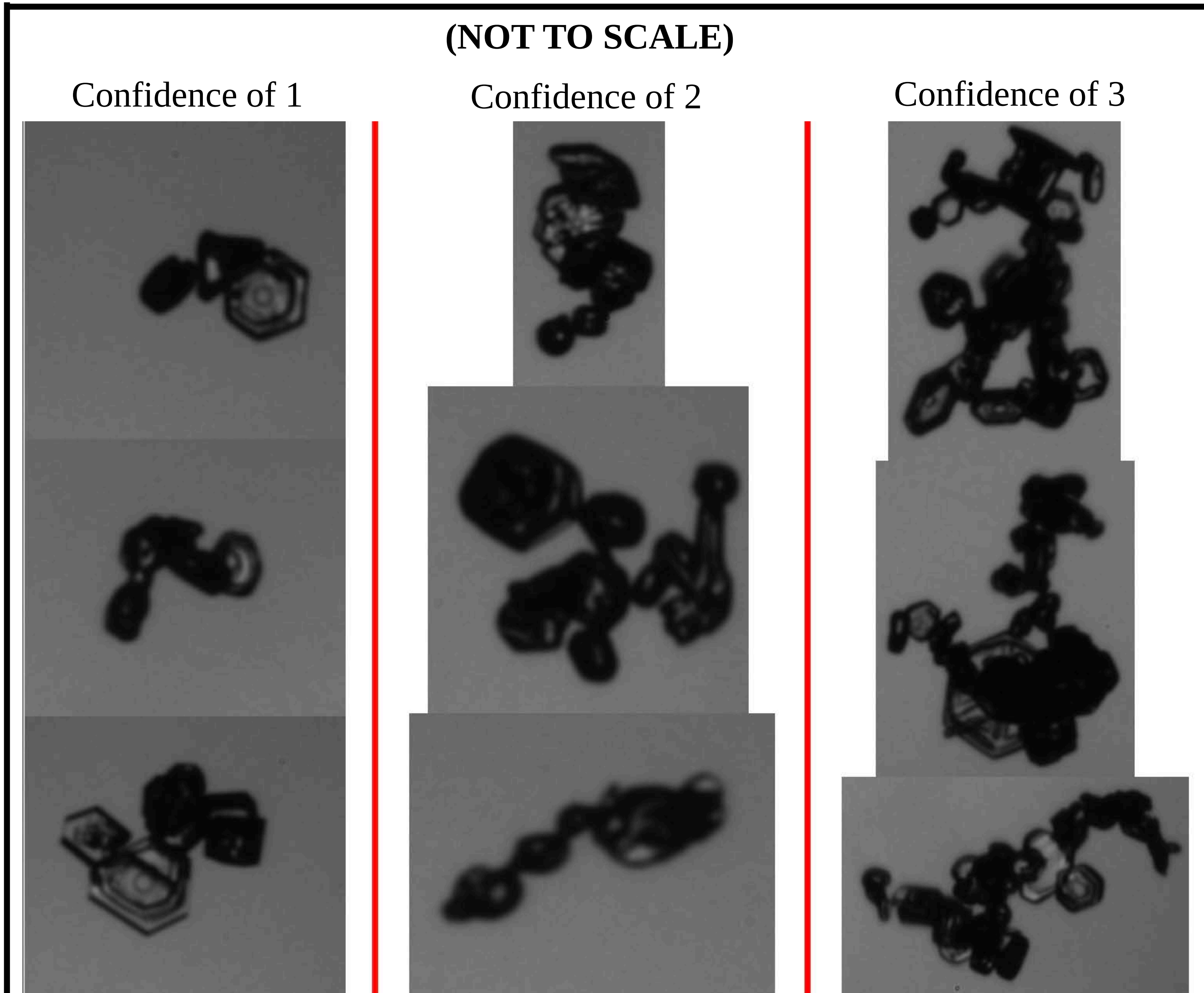

LROSE-TITAN

- Lidar Radar Open Software Environment software package (LROSE) Thunderstorm Identification Tracking And Nowcasting (TITAN)

- A 35 dBZ threshold is used to identify and track individual thunderstorms.

- Latitude and Longitude coordinates of the reflectivity centroid is computed by TITAN.

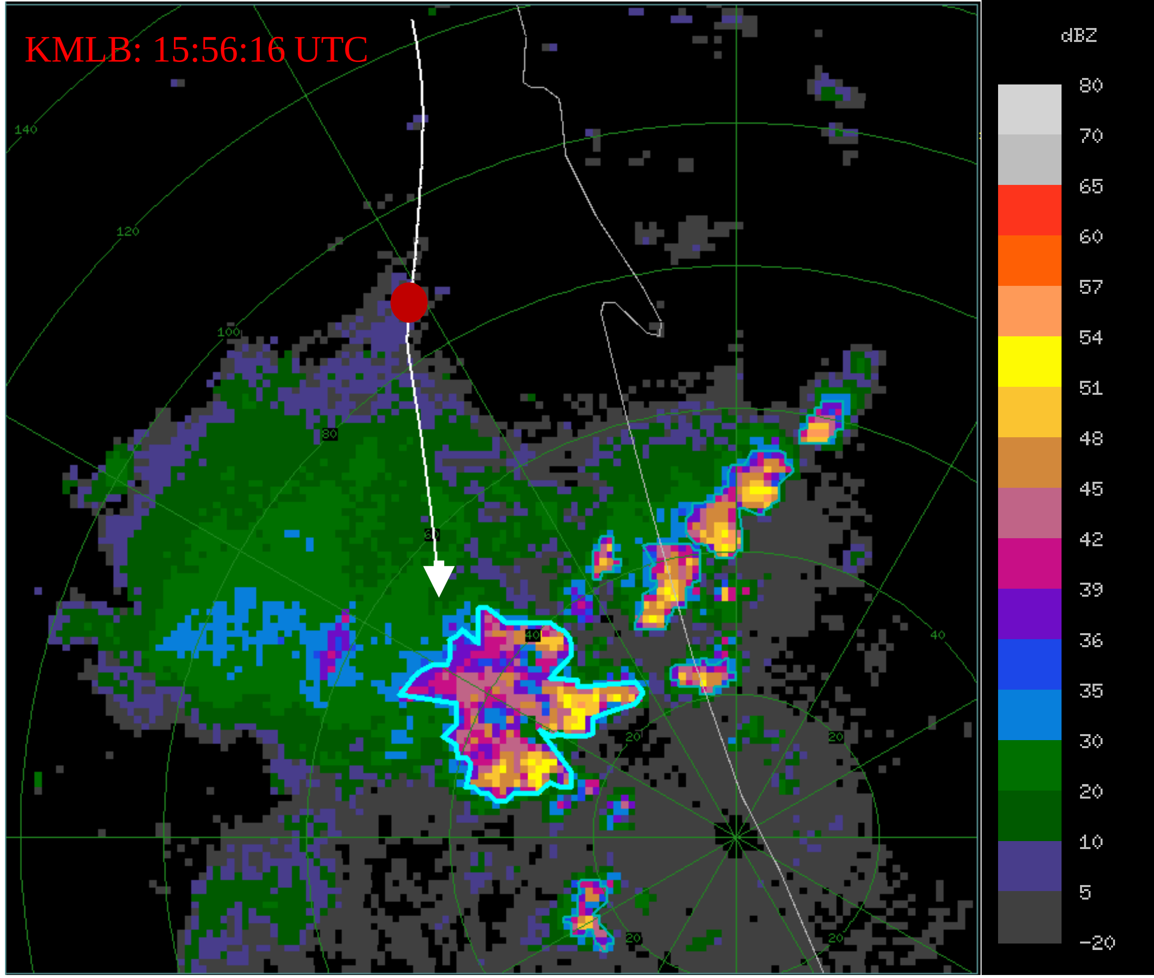

Composite radar reflectivity (dBZ) from the KMLB radar with TITAN cell tracking (blue outline).

Storm Evolution

- Deteriorating convection prior to 15:00 UTC.
- Cell is re-enhanced by a surface boundary at 15:00 UTC.
    - Electrically Active
- OST seen at 15:30 UTC.
- Aircraft sampling begins at 15:51:15 UTC
    - Ends at 16:26:00 UTC
- Storm merges with other initiated cells over Cape Canaveral, Florida at 16:30 UTC.
- Storms deteriorate over the Atlantic at 17:30 UTC.

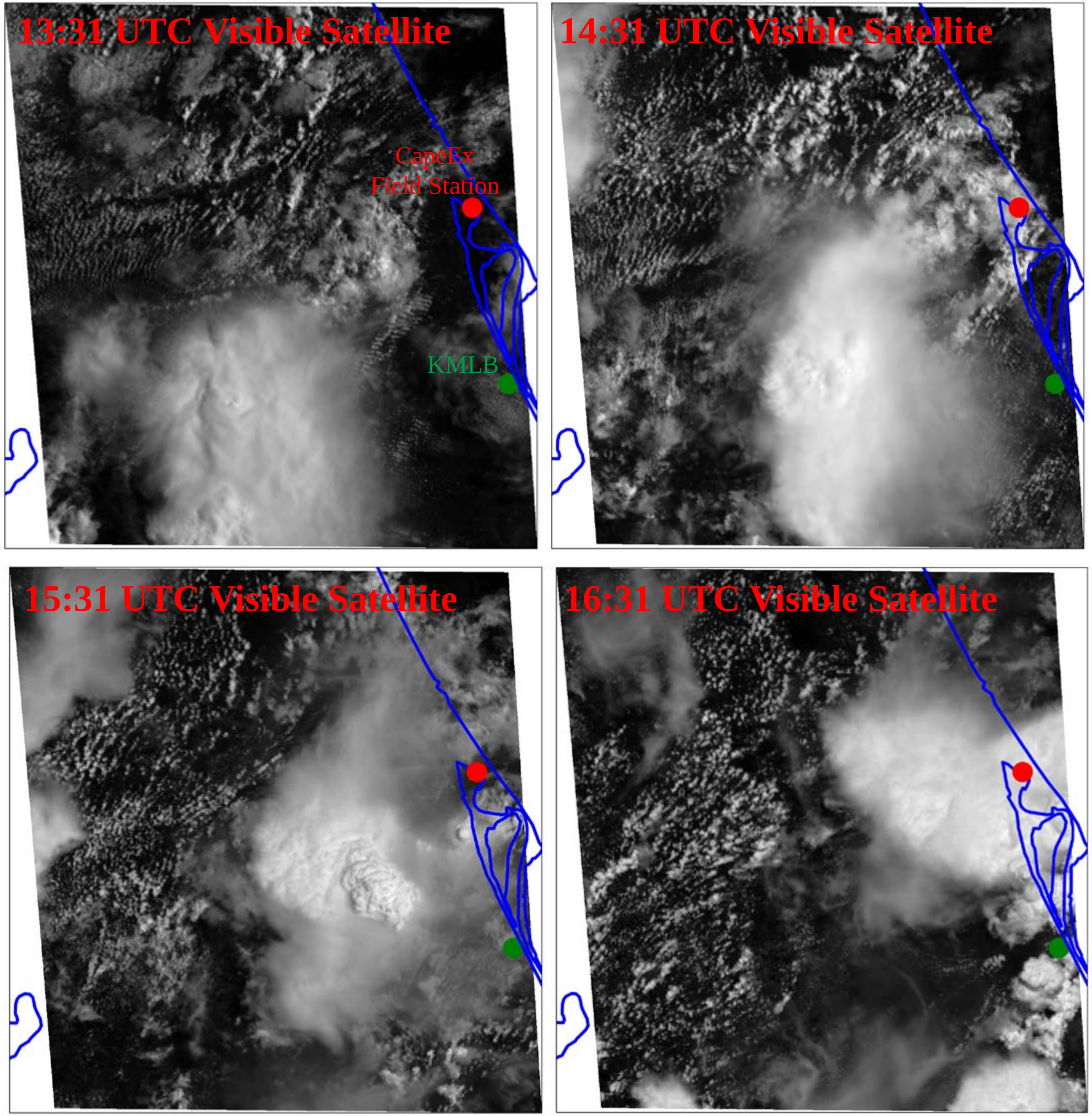

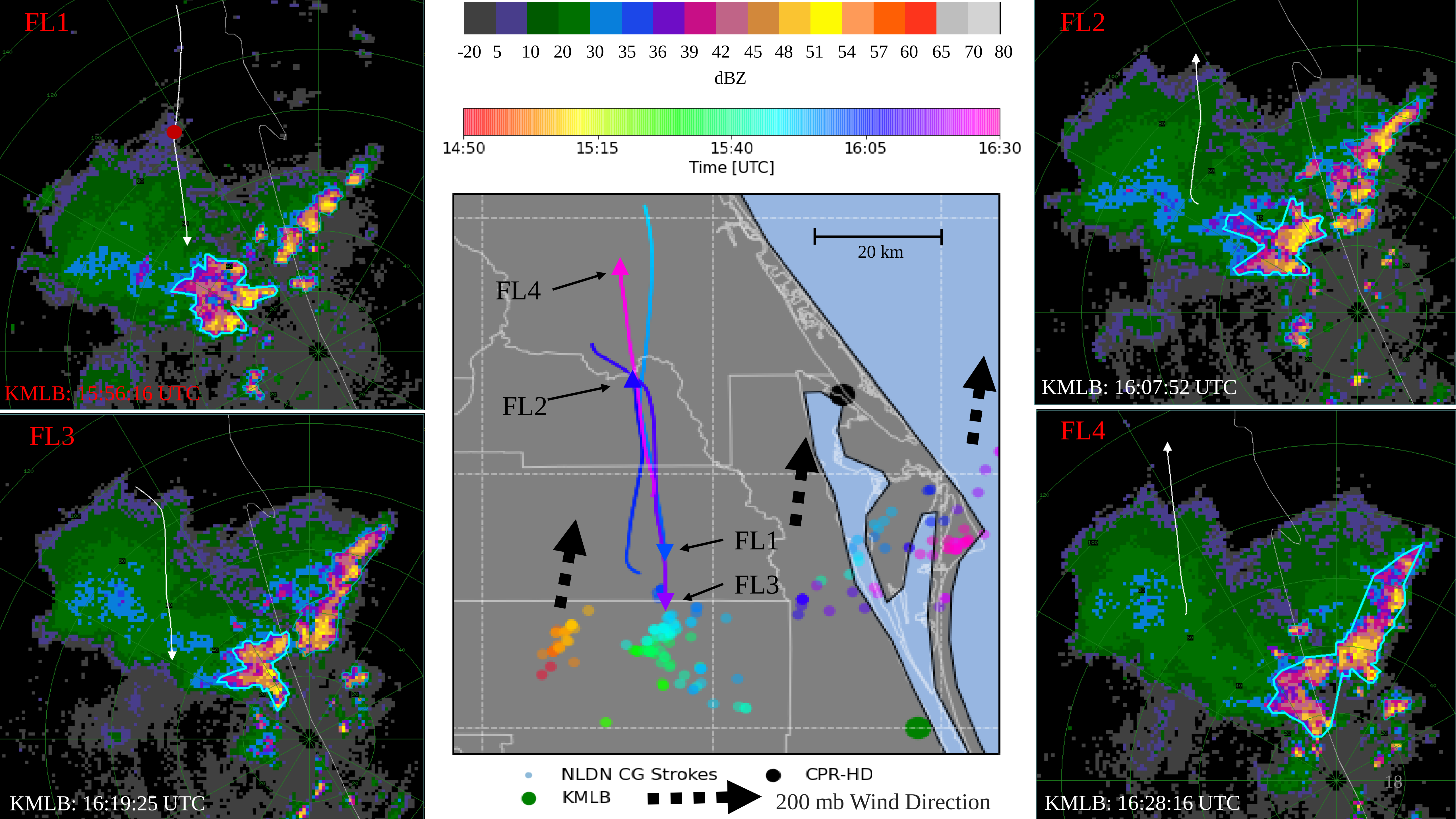

FL1
KMLB: 15:56:16 UTC
FL2
KMLB: 16:07:52 UTC
FL3
KMLB: 16:19:25 UTC
FL4
KMLB: 16:28:16 UTC
-20 5 10 20 30 35 36 39 42 45 48 51 54 57 60 65 70 80
dBZ
14:50 15:15 15:40 16:05 16:30
Time [UTC]
20 km
FL4
FL2
FL1
FL3
NLDN CG Strokes
CPR-HD
KMLB
200 mb Wind Direction

In-situ Microphysical Observations

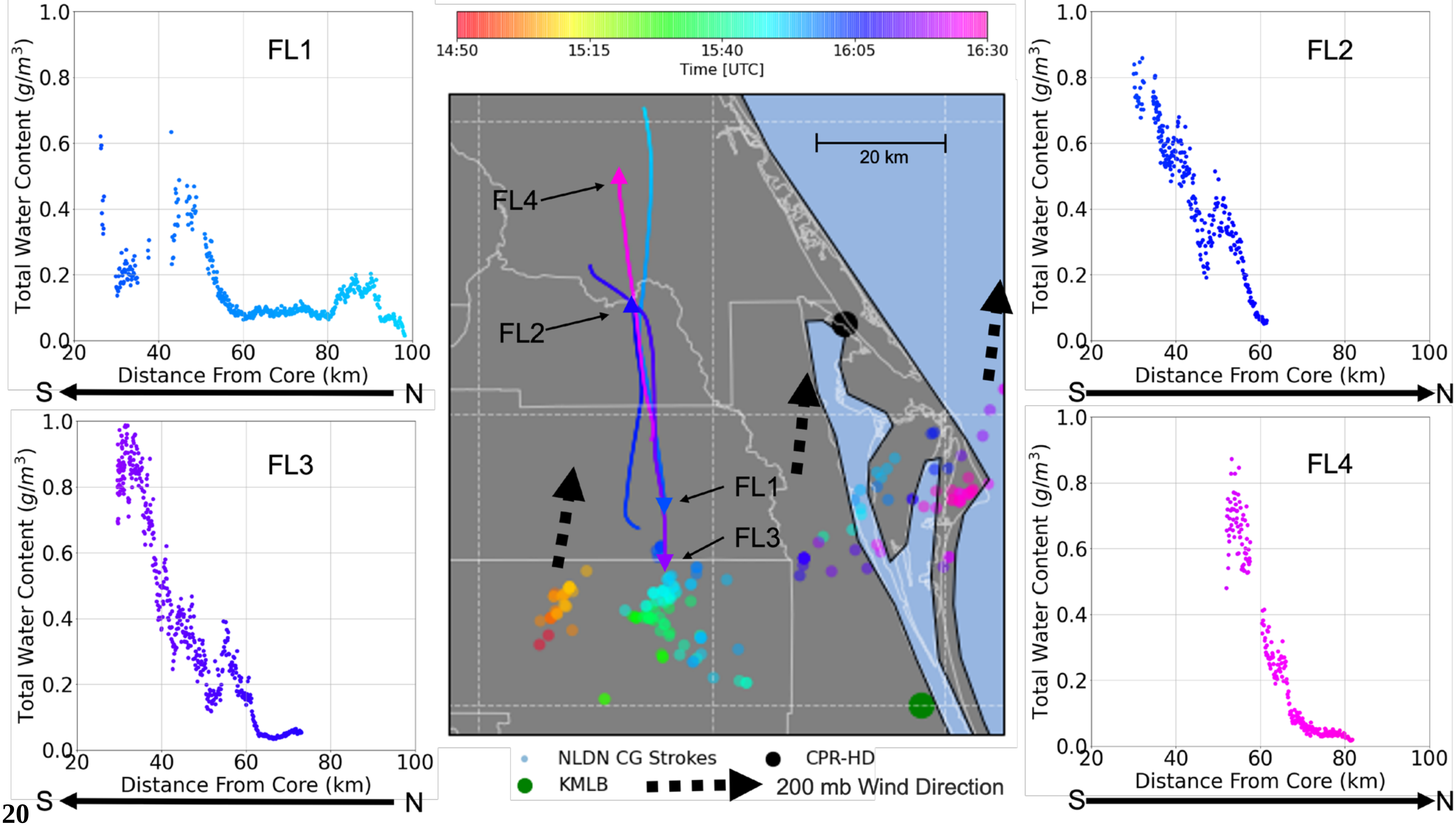
FL1
Total Water Content (g/m^3)
Distance From Core (km)
S
N
14:50
15:15
15:40
16:05
16:30
Time [UTC]
20 km
FL4
FL2
FL1
FL3
FL2
FL3
FL4
NLDN CG Strokes
CPR-HD
KMLB
200 mb Wind Direction

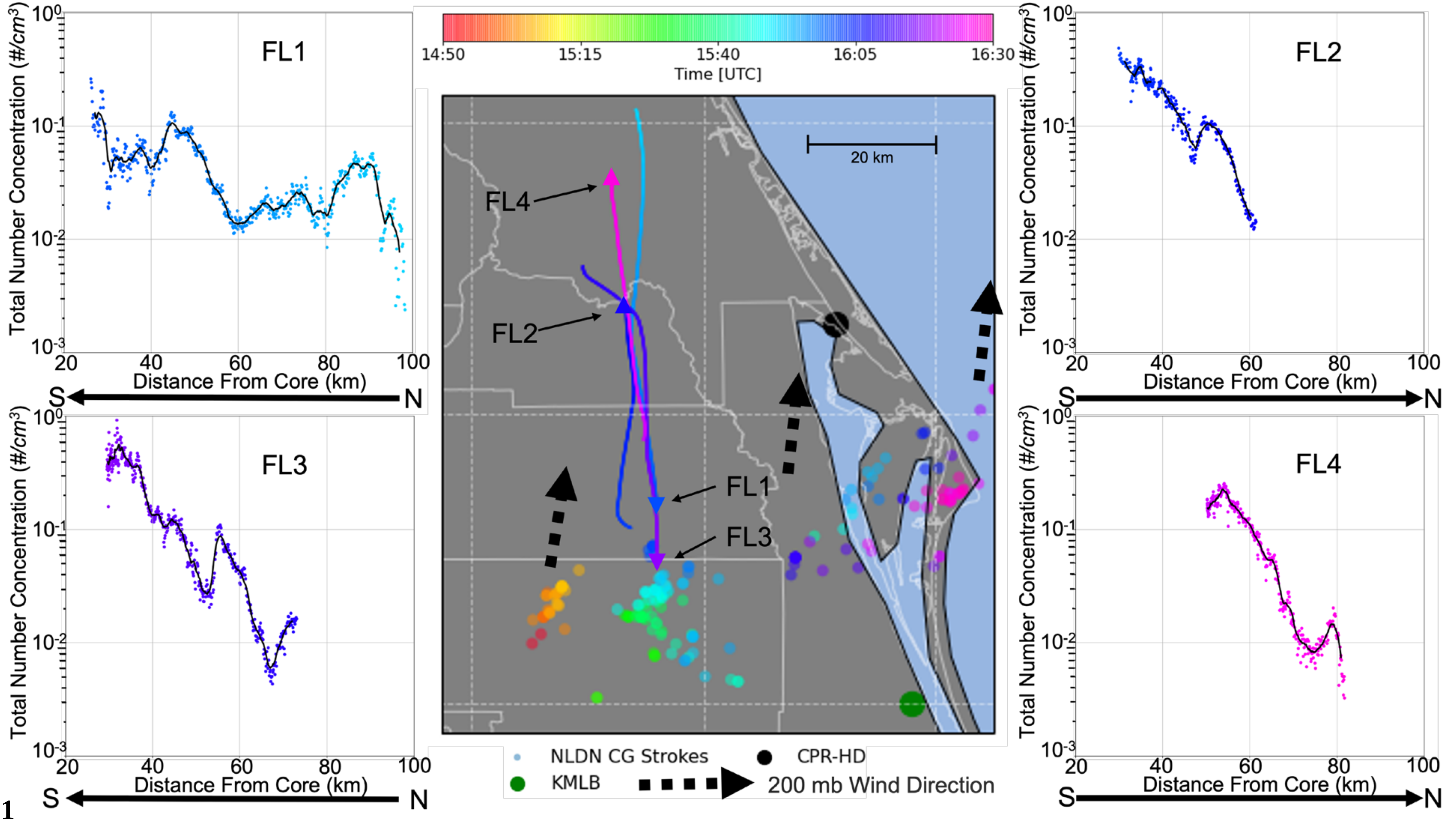
FL1
FL2
FL3
FL4
Total Number Concentration (#/cm³)
Distance From Core (km)
S
N
14:50
15:15
15:40
16:05
16:30
Time [UTC]
20 km
NLDN CG Strokes
CPR-HD
KMLB
200 mb Wind Direction

Observed Chain Aggregates (PHIPS)

- Complex Structures and Orientations

- Mostly consist of hexagonal plates, sectored plates, columns, and capped columns.

- Only 10% (N = 66) contained some evidence of riming.

- Signs of sublimation of the chains far from the storm core (40 to 100 km).

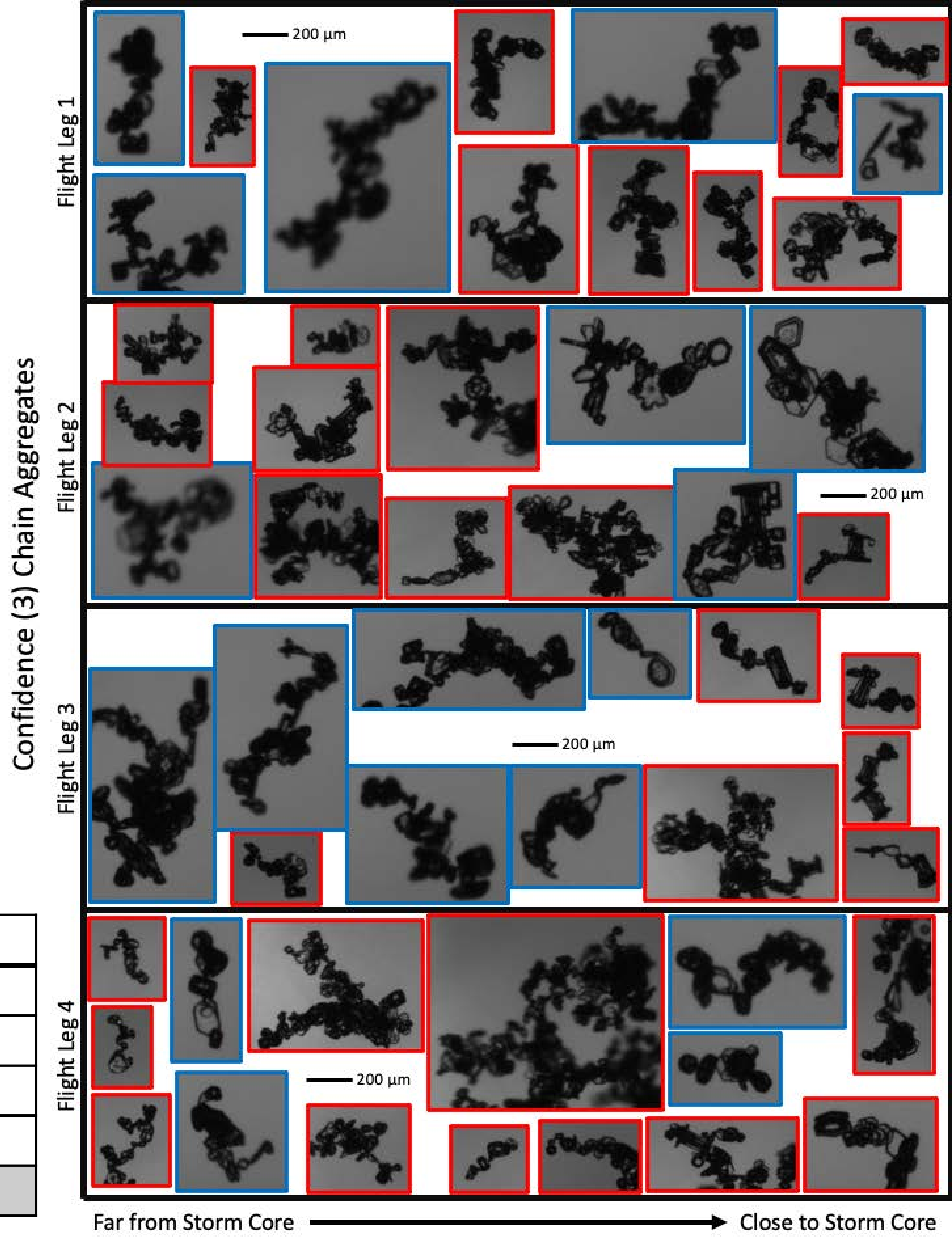

Legs	Number of Images	Confidence of 1	Confidence of 2	Confidence of 3	All Confidences
FL1	1,507	4.6 (N=69)	5.3 (N=80)	4.6 (N=69)	14.5 (N=218)
FL2	917	4.3 (N=39)	5.2 (N=48)	3.4 (N=31)	12.9 (N=118)
FL3	1,375	4.7 (N=64)	6.5 (N=89)	2.8 (N=38)	13.9 (N=191)
FL4	855	4.0 (N=33)	7.7 (N=67)	4.8 (N=41)	16.5 (N=141)
TOTAL	**4,654**	**4.4 (N=205)**	**6.1 (N=284)**	**3.8 (N=179)**	**14.4 (N=668)**

Chain Aggregates vs. Distance from Core

- Highest concentrations are between 70 and 100 km from the TITAN cell's core (16.2%).

- Smallest concentrations are between 10 and 40 km from the TITAN cell's core (10%).

- Highest number of chains observed between 40 and 70 km from the TITAN cell's core.

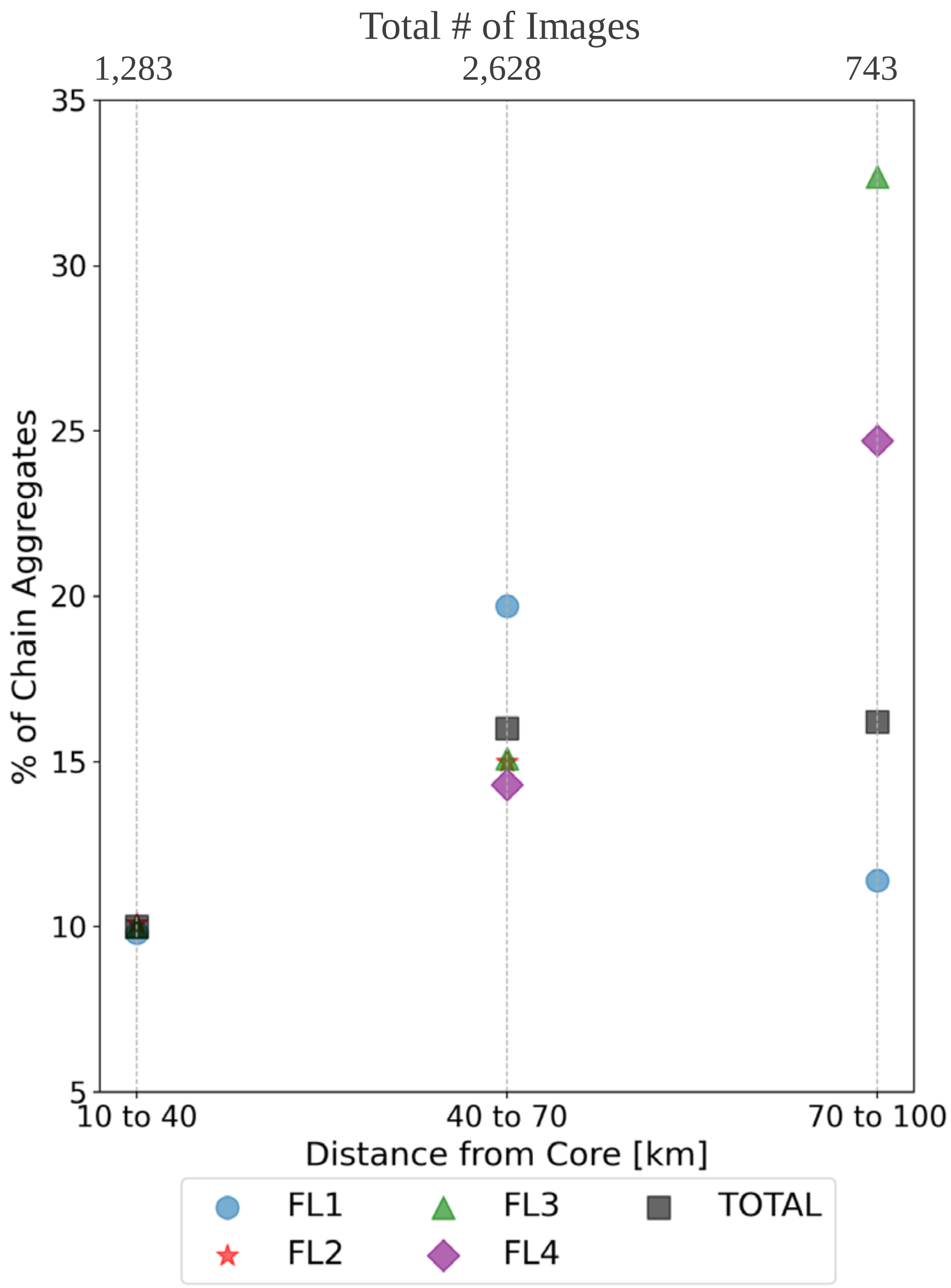

‘All In’ Chain Aggregate Sizes

- Sizes (max diameter) range from approximately 150 to 800 μm.

- Average 25th Percentile = 293 μm
- Average 50th Percentile = 367 μm
- Average 75th Percentile = 458 μm

- The size distribution of the chain aggregates is similar between FL1-4.
  – Indicating that storm evolution does not impact chain aggregate sizes.

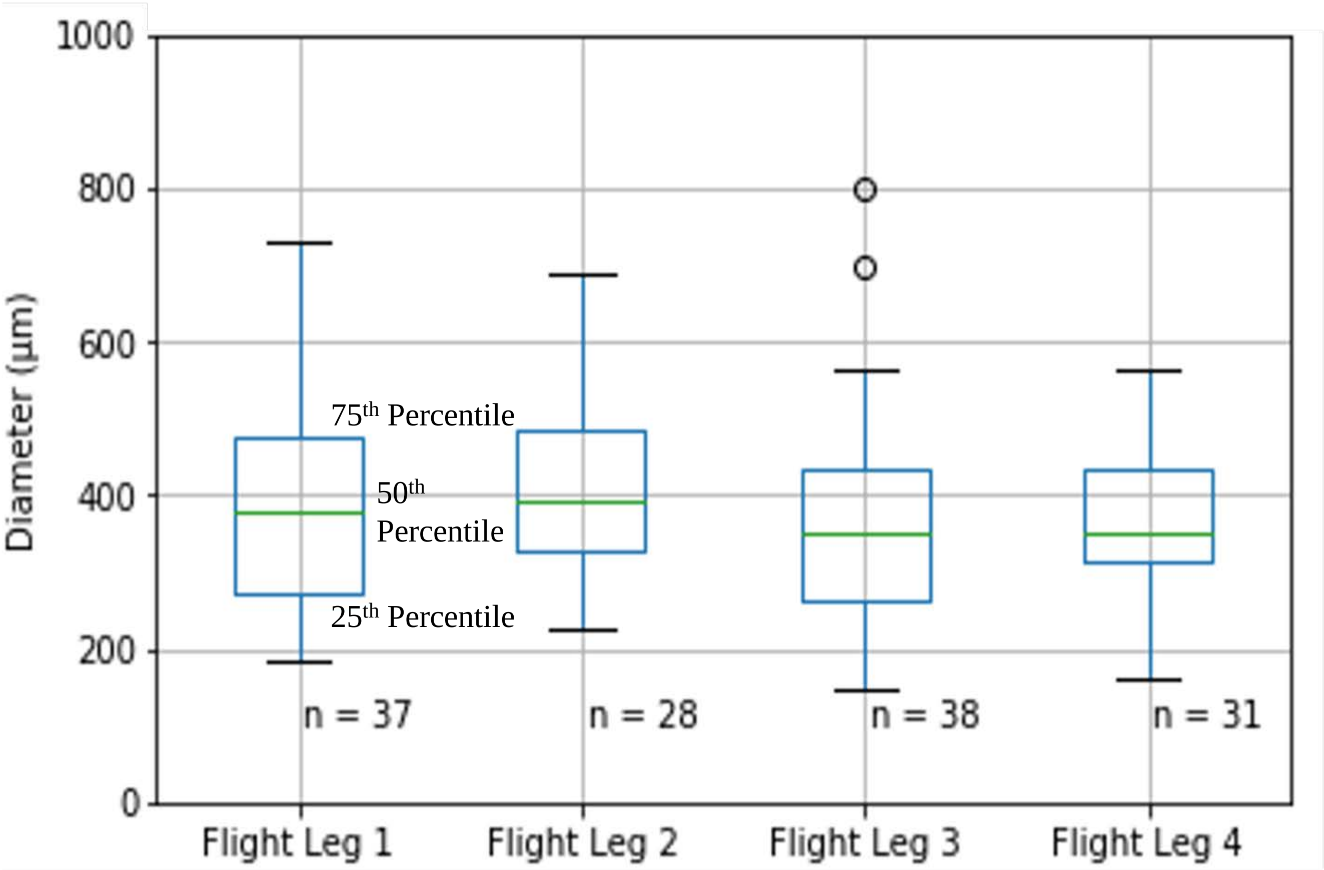

Box and whisker plot depicting ‘all in’ chain aggregate sizes (max diameter) measured by the PHIPS per flight leg with a moderate-to-high level of confidence.

PHIPS Chain Aggregate Percentiles

Legs	Particles > 495 μm	Chains > 495 μm	Chain Percentage	Confidence
FL1	7	7	100%	2.71
FL2	11	8	73%	2.38
FL3	8	7	88%	2.00
FL4	10	8	80%	1.88
TOTAL	**36**	**30**	**83%**	**2.24**

- Found that 83% of particles > 495 μm imaged by the PHIPS are chain aggregates.
  - With an average confidence between moderate and high (2.24).

- Found that 9.5% of particles between 105 and 315 μm imaged by the PHIPS are chain aggregates (not in table).
  - With an average confidence between low and moderate (1.38).

PHIPS Chains to CIP Concentrations

- Simplifications:

– **Particles > 495 μm** measured by the CIP is considered the **chain aggregate concentration**.

– **Particles between 105-315 μm** is the **non-chain aggregate concentration**.

– **Particles between 315-495 μm** is the **buffer zone** between the two concentrations.

UNIVERSITY OF NORTH DAKOTA

Concentrations

- More non-chain aggregates than chain aggregates.
- Highest chain aggregate concentrations nearest to core.
    - Except for FL1
- Convergence between the chain and non-chain aggregate concentrations.
- **NOTE**: Points of convergence are never at the closest point to the storm core!

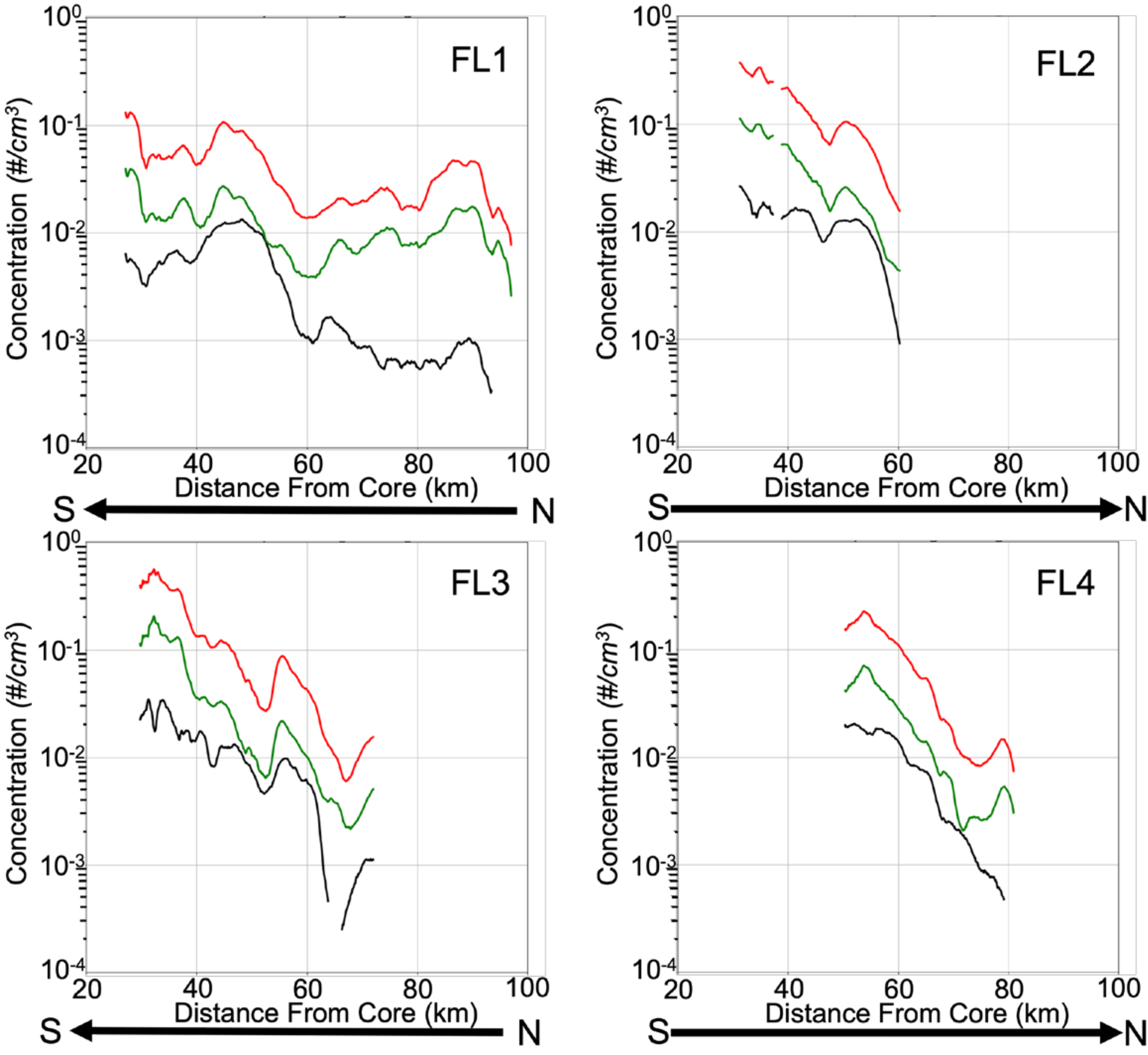

— Chain Aggregate Concentration — Non-chain Aggregate Concentration — Total Number Concentration

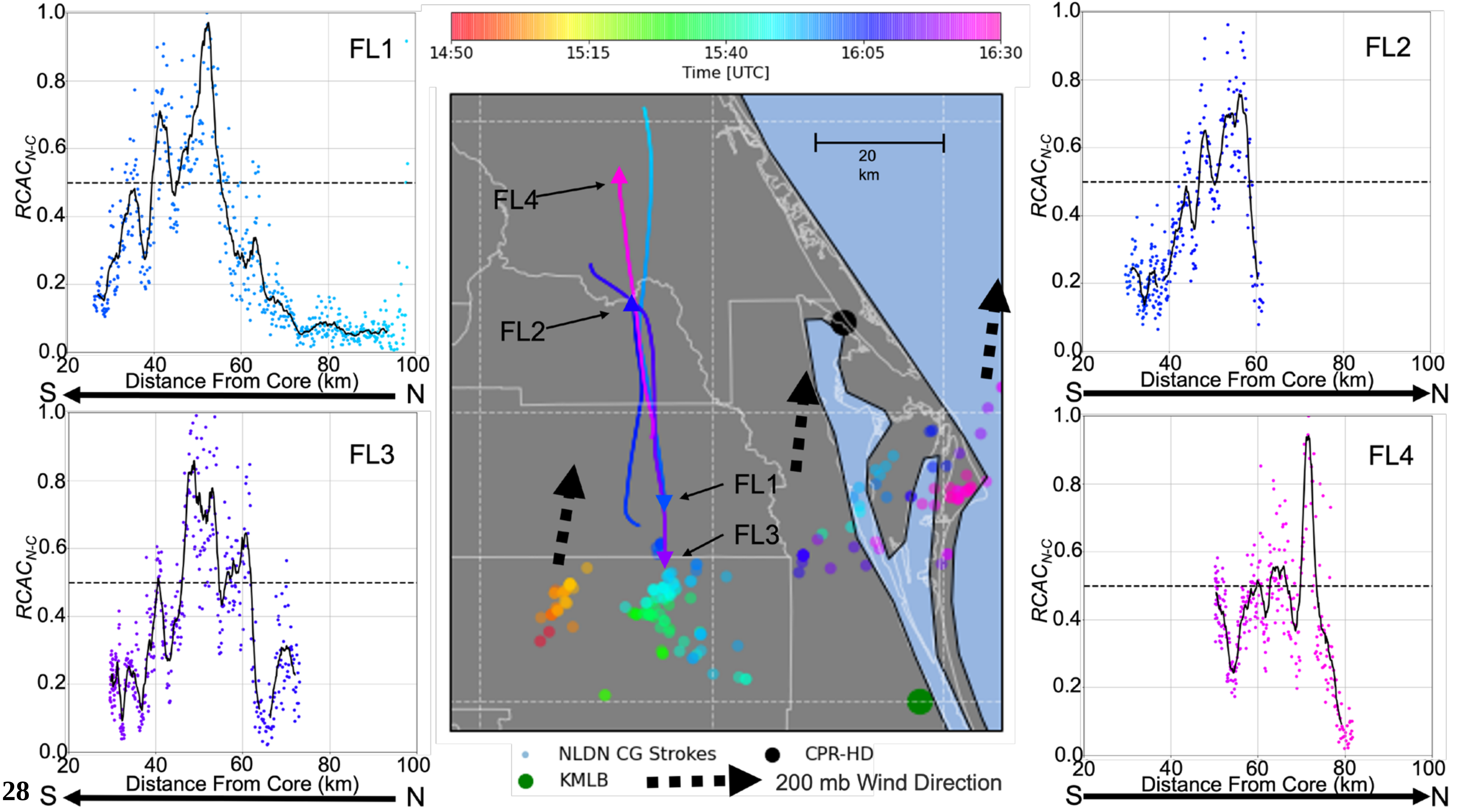

14:50
15:15
15:40
16:05
16:30
Time [UTC]
FL1
FL2
FL3
FL4
20 km
$RCAC_{N\text{-}C}$
Distance From Core (km)
S
N
NLDN CG Strokes
CPR-HD
KMLB
200 mb Wind Direction

Electrical Field Observations

Electric Field Observations

- All flight legs have electric field magnitude (E_{mag}) on the order of 10^1 kV m^{-1}
- Strongest in relatively close proximity to the TITAN cell's core
- FL1 (E_z peaked at -22.37 kV m^{-1})
- Do not reach 60 kV m^{-1} Threshold

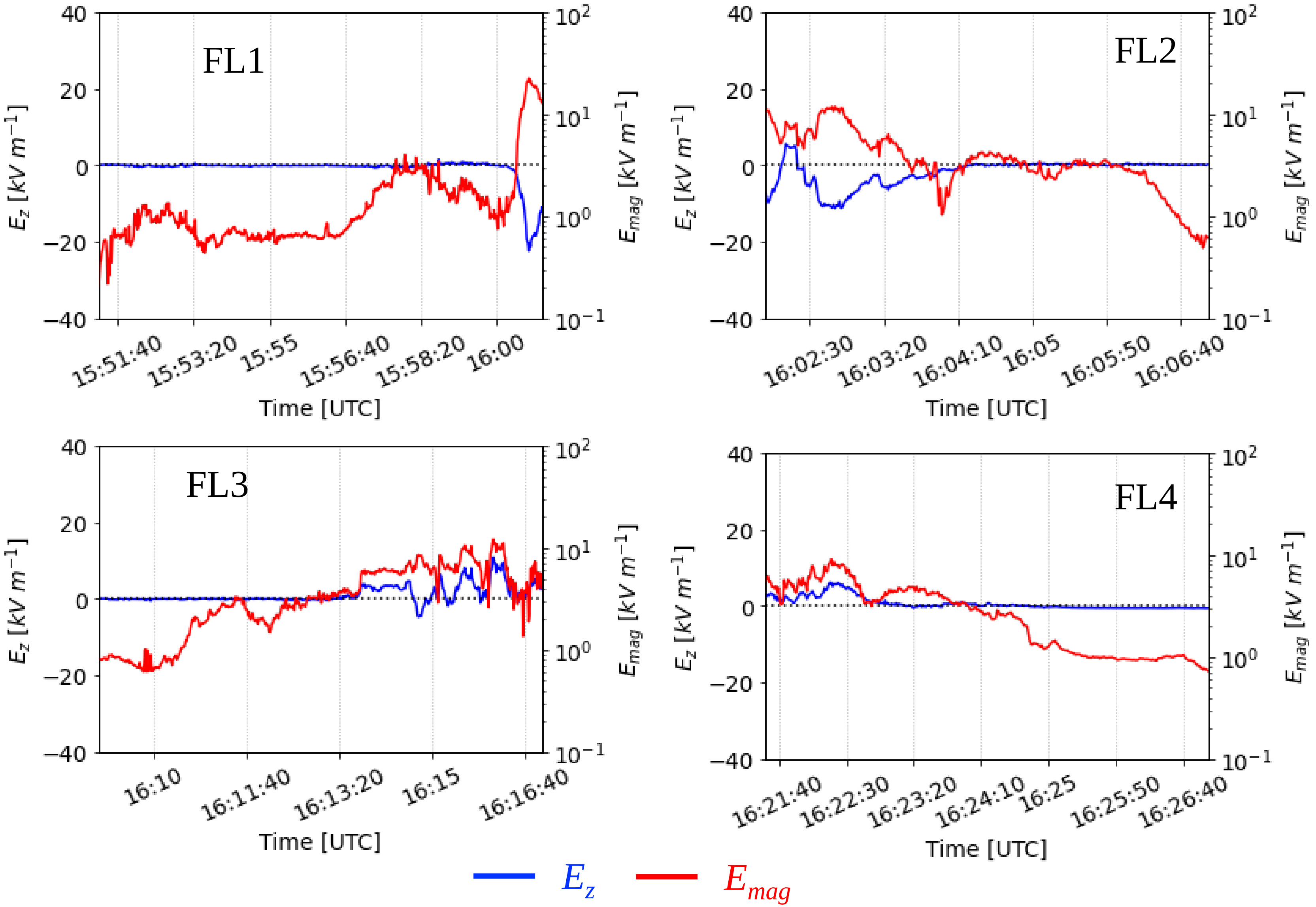

Radar and Satellite

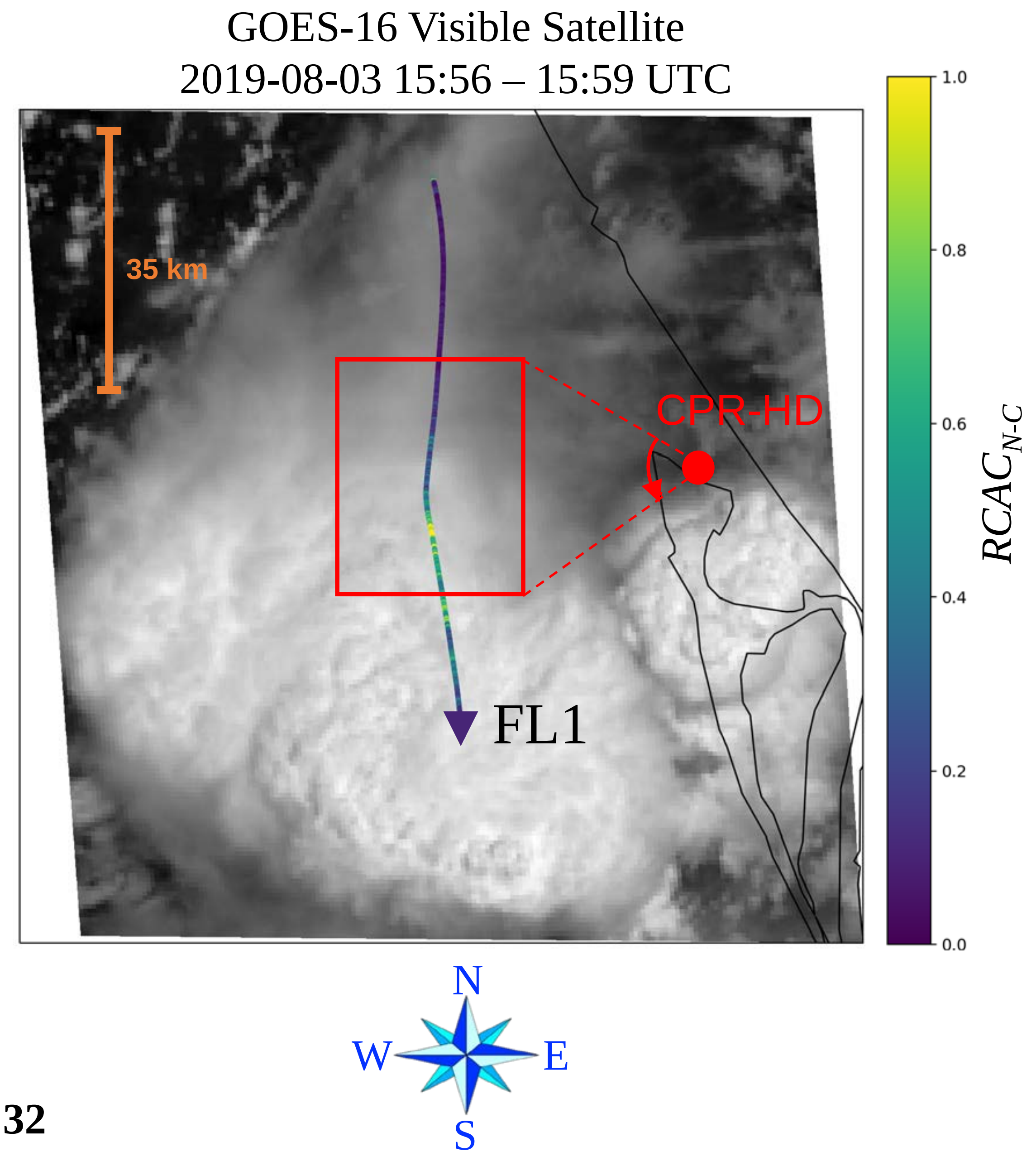
GOES-16 Visible Satellite
2019-08-03 15:56 – 15:59 UTC
35 km
CPR-HD
FL1
1.0
0.8
0.6
0.4
0.2
0.0
$RCAC_{N\text{-}C}$
N
W
E
S

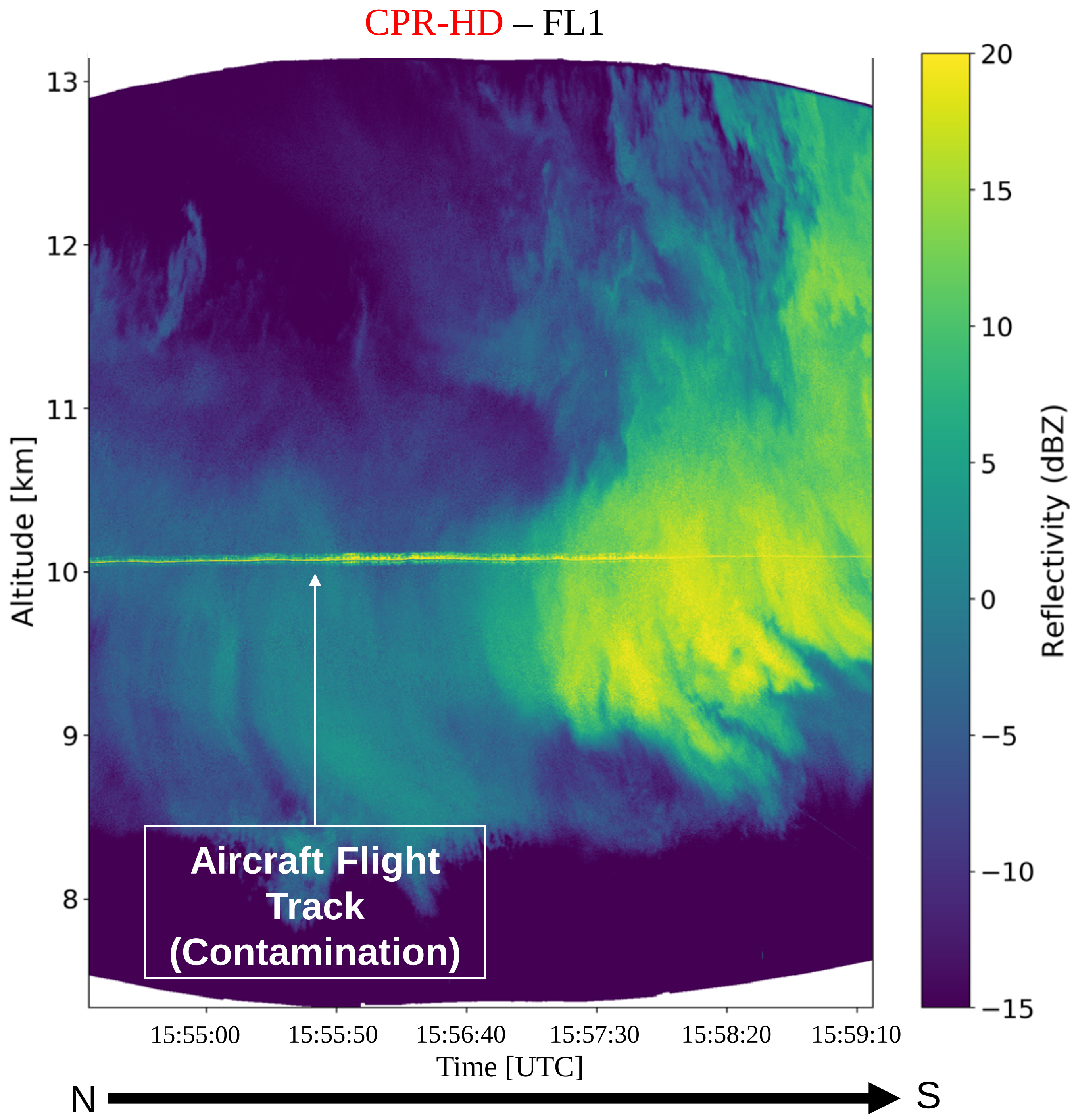
CPR-HD – FL1
Altitude [km]
13
12
11
10
9
8
Aircraft Flight Track (Contamination)
15:55:00
15:55:50
15:56:40
15:57:30
15:58:20
15:59:10
Time [UTC]
Reflectivity (dBZ)
20
15
10
5
0
−5
−10
−15
N
S

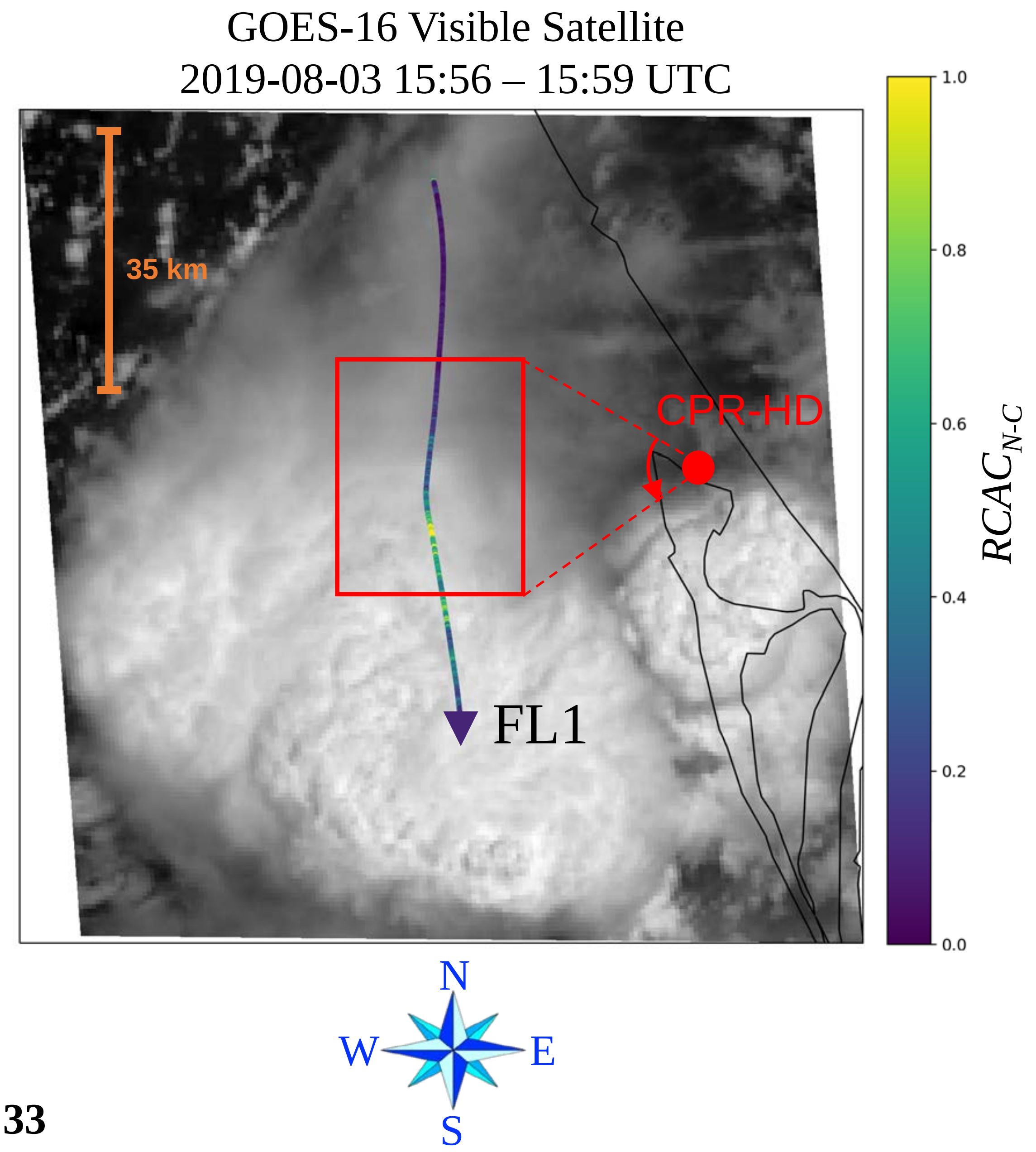
GOES-16 Visible Satellite
2019-08-03 15:56 – 15:59 UTC
35 km
CPR-HD
FL1
$RCAC_{N\text{-}C}$
1.0
0.8
0.6
0.4
0.2
0.0
N
W
E
S

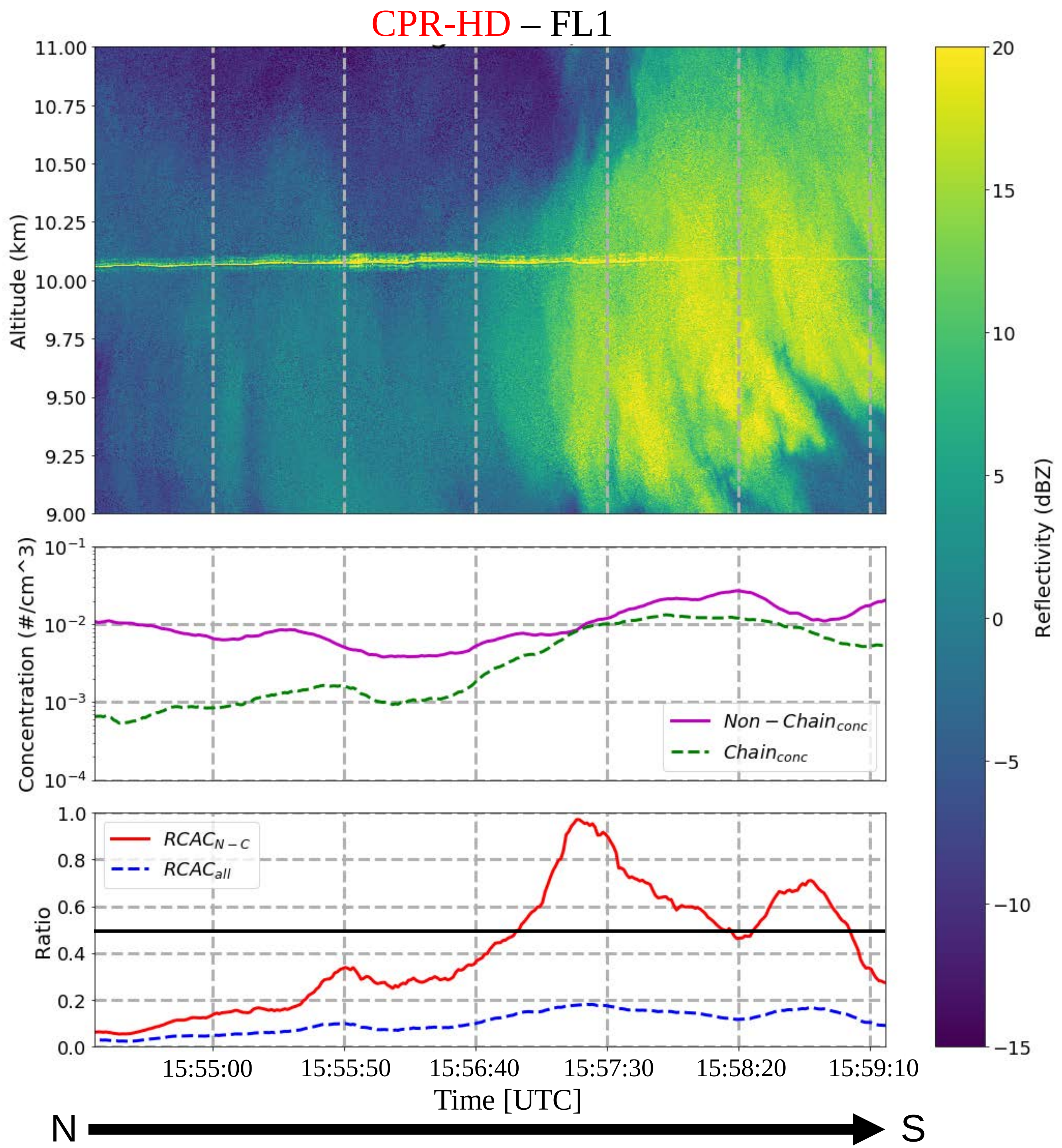
CPR-HD – FL1
Altitude (km)
Reflectivity (dBZ)
Concentration (#/cm^3)
Non – Chain$_{conc}$
Chain$_{conc}$
Ratio
$RCAC_{N-C}$
$RCAC_{all}$
15:55:00
15:55:50
15:56:40
15:57:30
15:58:20
15:59:10
Time [UTC]
N
S

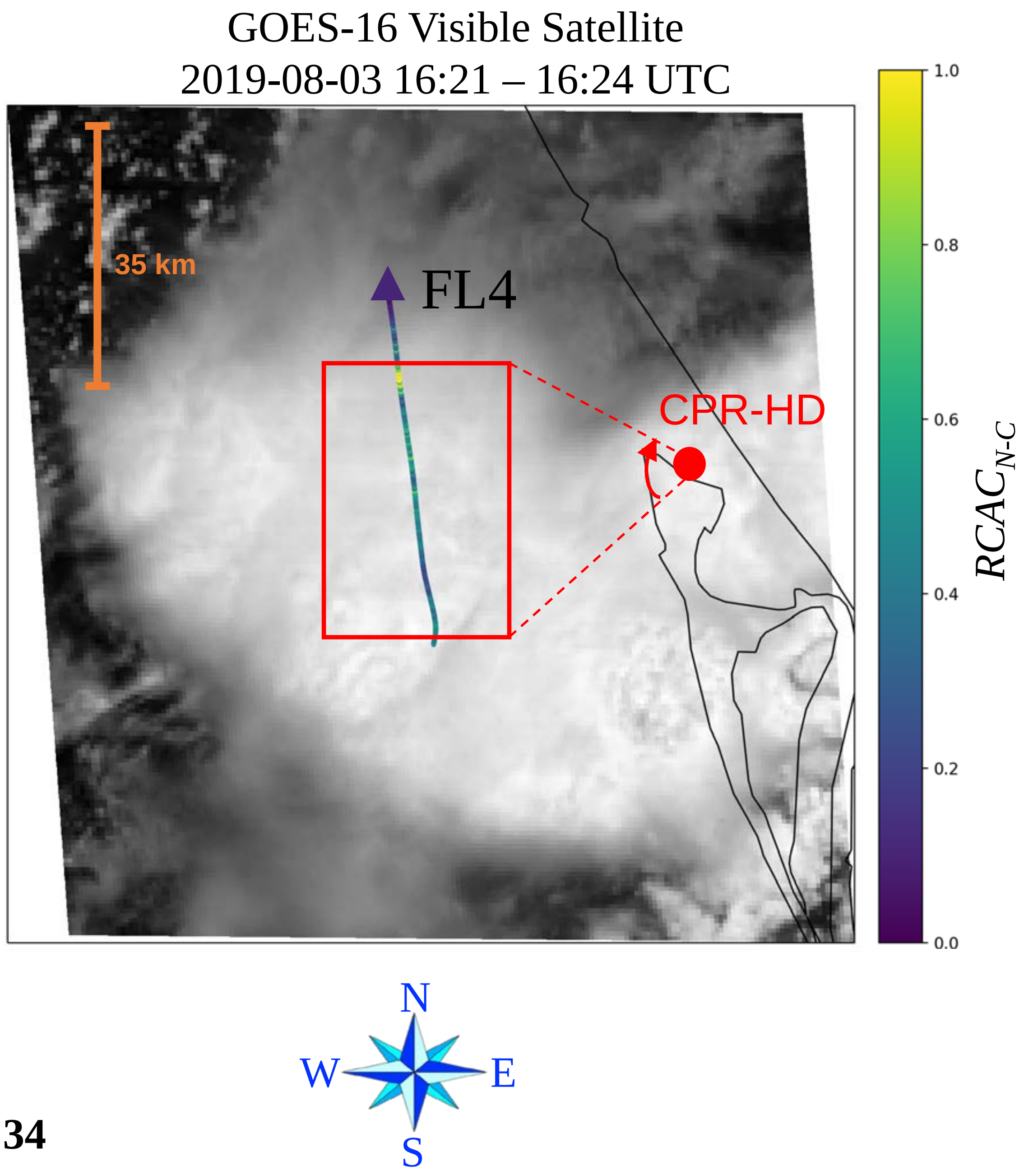
GOES-16 Visible Satellite
2019-08-03 16:21 – 16:24 UTC
35 km
FL4
CPR-HD
$RCAC_{N\text{-}C}$
1.0
0.8
0.6
0.4
0.2
0.0
N
W
E
S

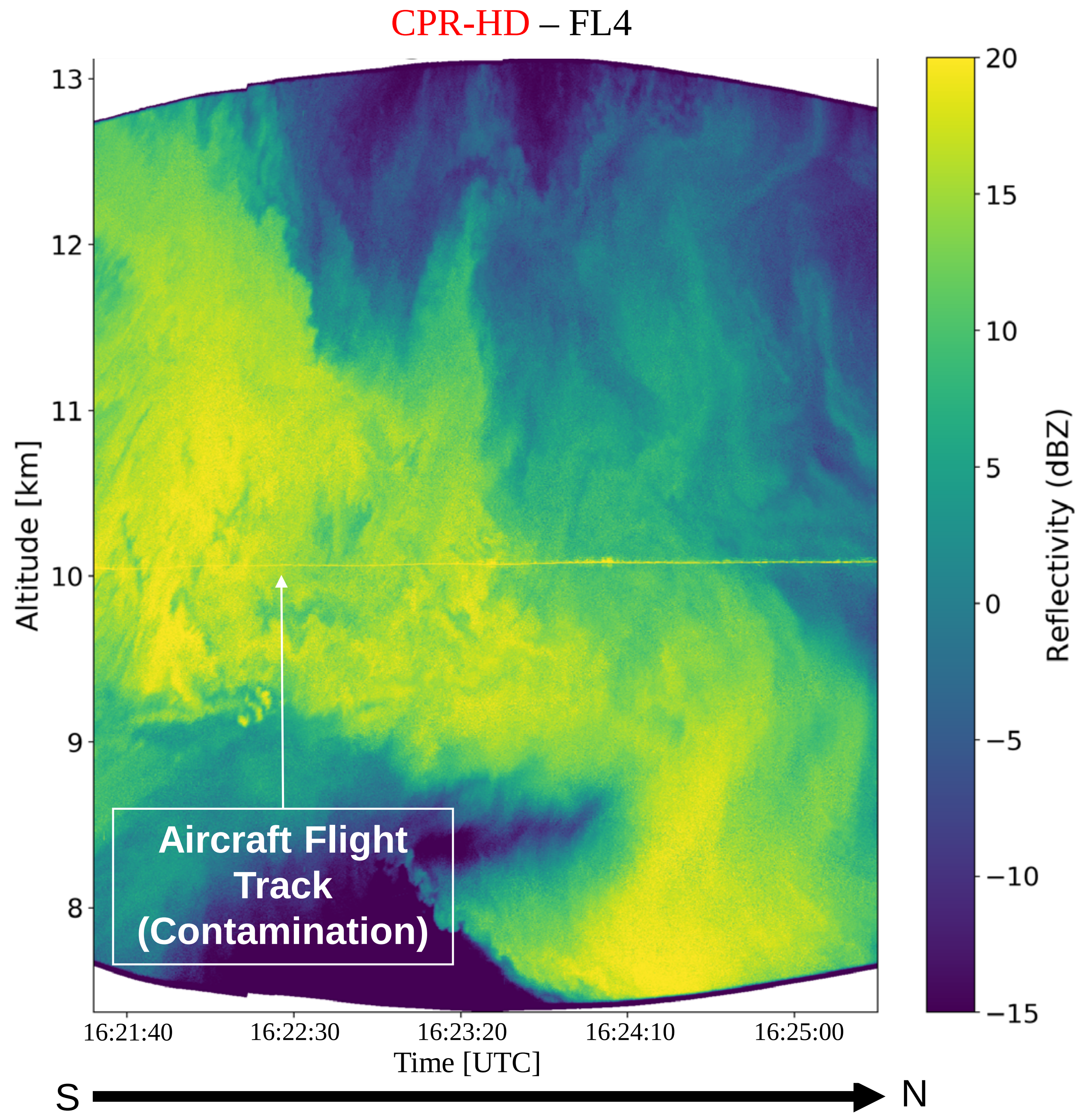
CPR-HD – FL4
Altitude [km]
13
12
11
10
9
8
Aircraft Flight Track (Contamination)
16:21:40
16:22:30
16:23:20
16:24:10
16:25:00
Time [UTC]
Reflectivity (dBZ)
20
15
10
5
0
−5
−10
−15
S
N

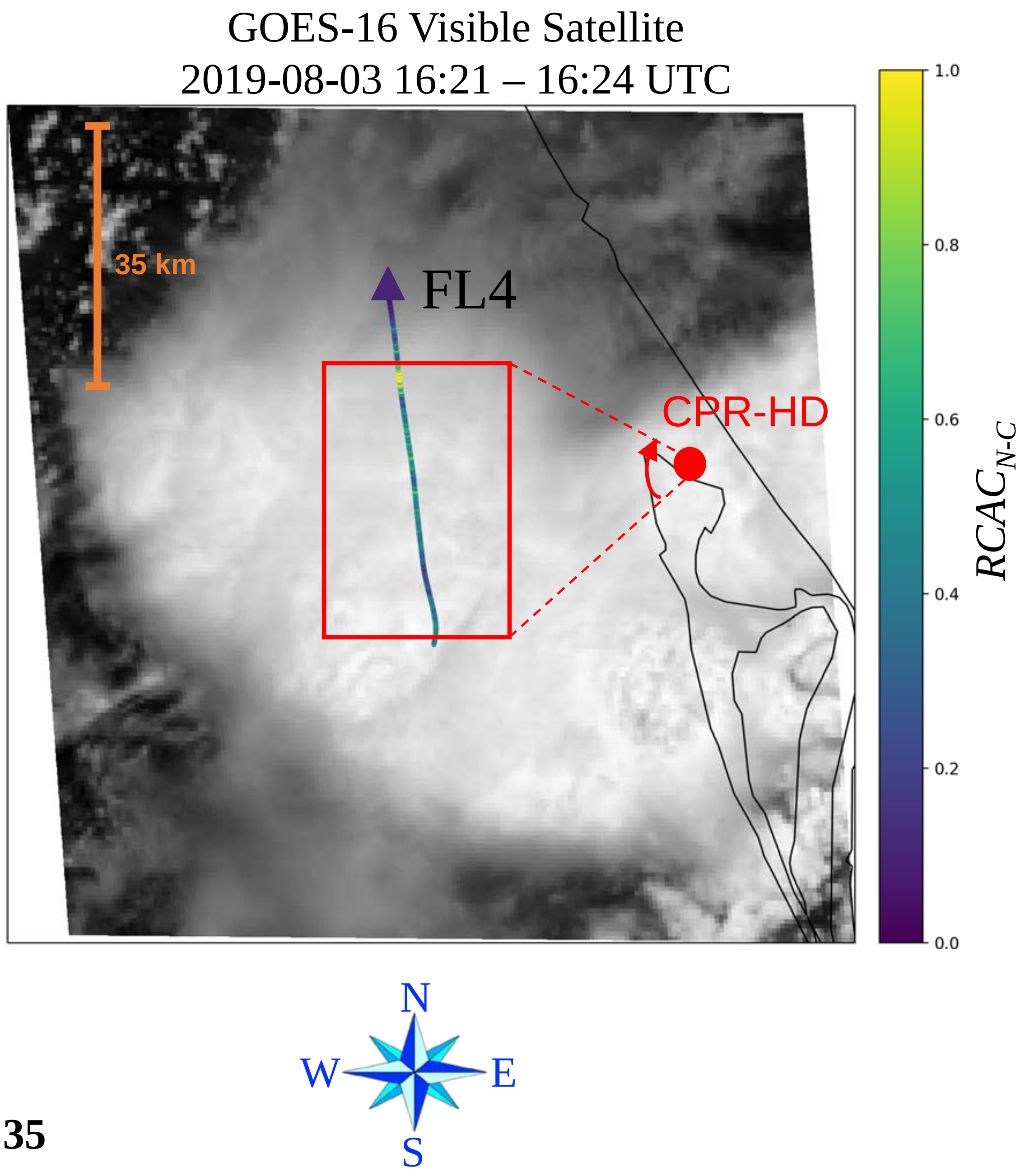
GOES-16 Visible Satellite
2019-08-03 16:21 – 16:24 UTC
35 km
FL4
CPR-HD
RCAC$_{N\text{-}C}$
1.0
0.8
0.6
0.4
0.2
0.0
N
W
E
S

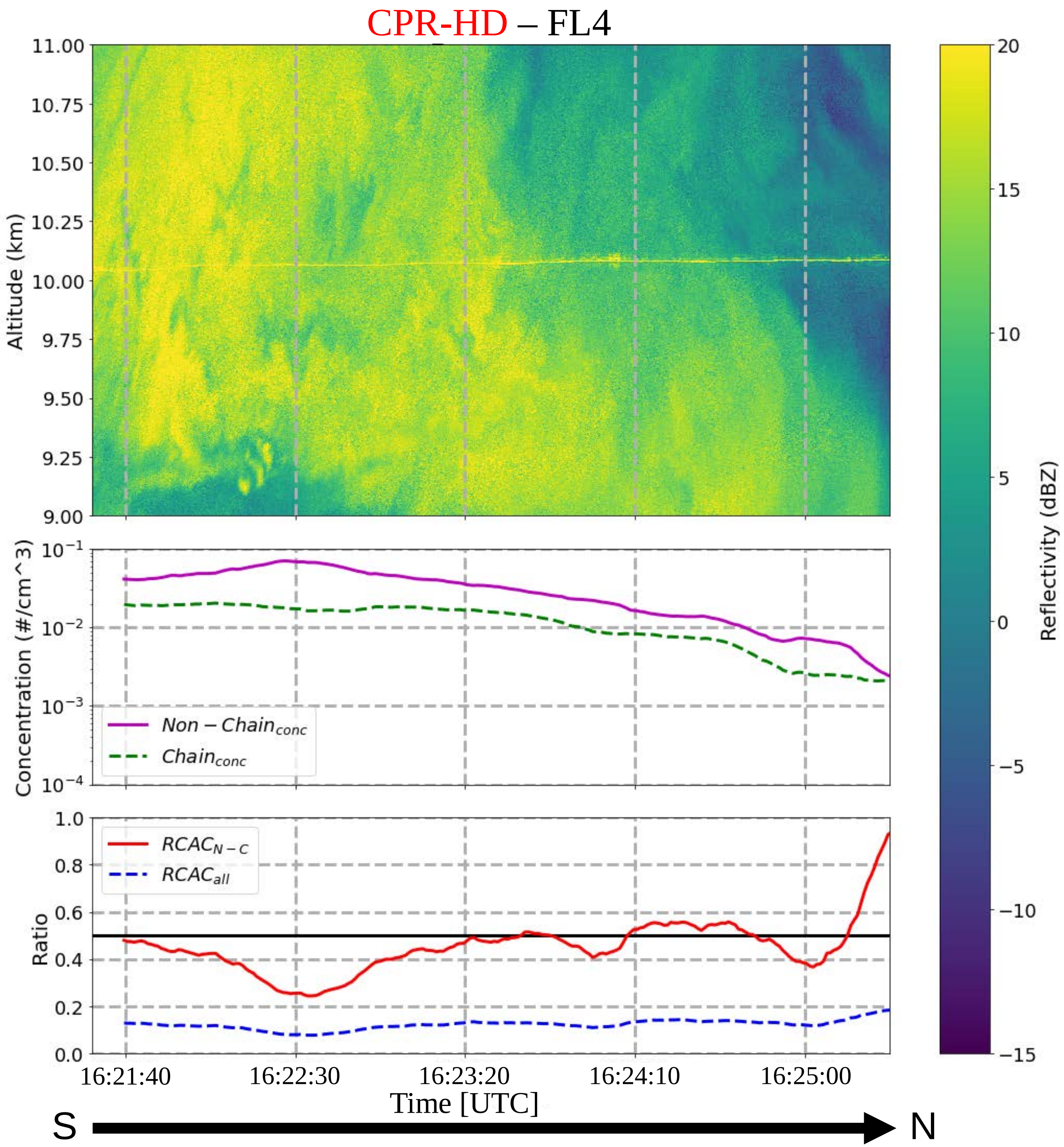
CPR-HD – FL4
Altitude (km)
11.00
10.75
10.50
10.25
10.00
9.75
9.50
9.25
9.00
Reflectivity (dBZ)
20
15
10
5
0
−5
−10
−15
Concentration (#/cm^3)
10^{-1}
10^{-2}
10^{-3}
10^{-4}
$Non-Chain_{conc}$
$Chain_{conc}$
Ratio
1.0
0.8
0.6
0.4
0.2
0.0
$RCAC_{N-C}$
$RCAC_{all}$
16:21:40
16:22:30
16:23:20
16:24:10
16:25:00
Time [UTC]
S
N

Conclusions

- Chain aggregates show similar complexity to previous experiments.
  - 14.4% of PHIPS images classified as chain aggregates.

- Flight leg 1 provides evidence that chain aggregation is occurring in the main convective region of the storm.
  - Highest $RCAC_{N\text{-}C}$ near storm core at boundary between old and new cirrus anvil.
  - Lack of sublimated particle elements.
  - Particle elements from different temperature regimes (-5 to -40 °C).
  - Lack of rimed chains – suggesting aggregation above the homogenous freezing level.

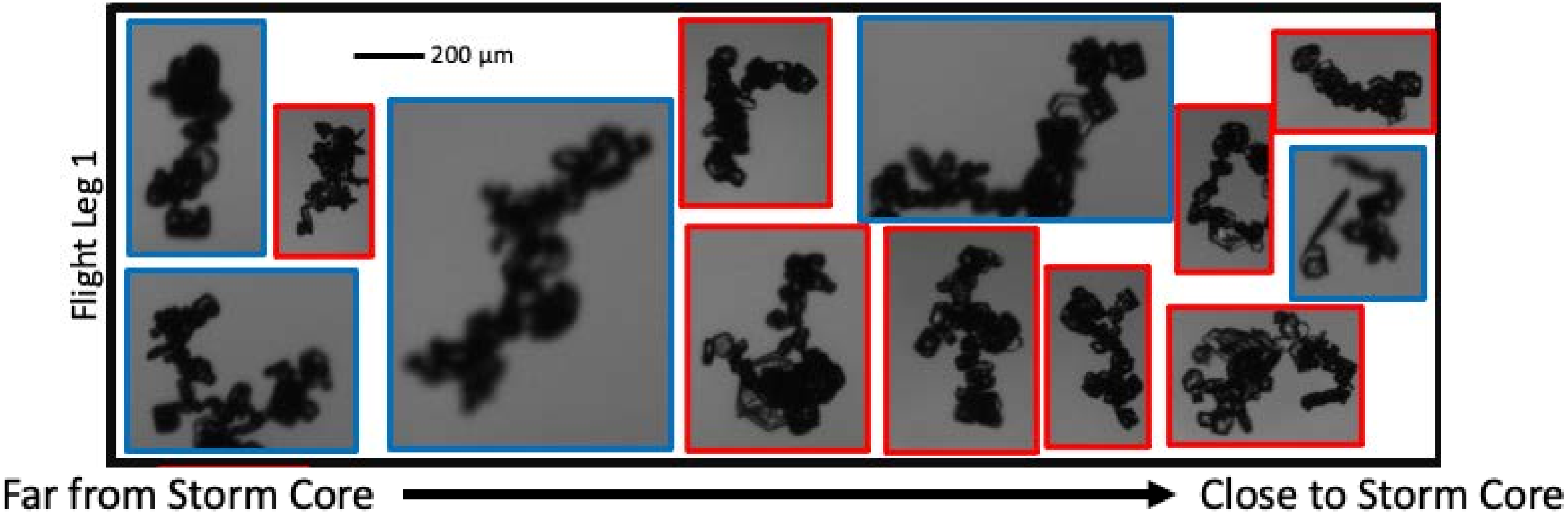

Conclusions

- Flight legs 2-4 provides evidence that chain aggregation is **continuing** in the cirrus anvil.
  - Positive slope of the $RCAC_{N\text{-}C}$ heading away from the storm core as overall concentrations decrease.

- Electric field strengths **never** surpass the laboratory tested threshold for chain aggregation to occur (60 kV m^{-1})
  - Strongest near the core
  - (Maximum E_{mag}: 22.5 kV m^{-1})

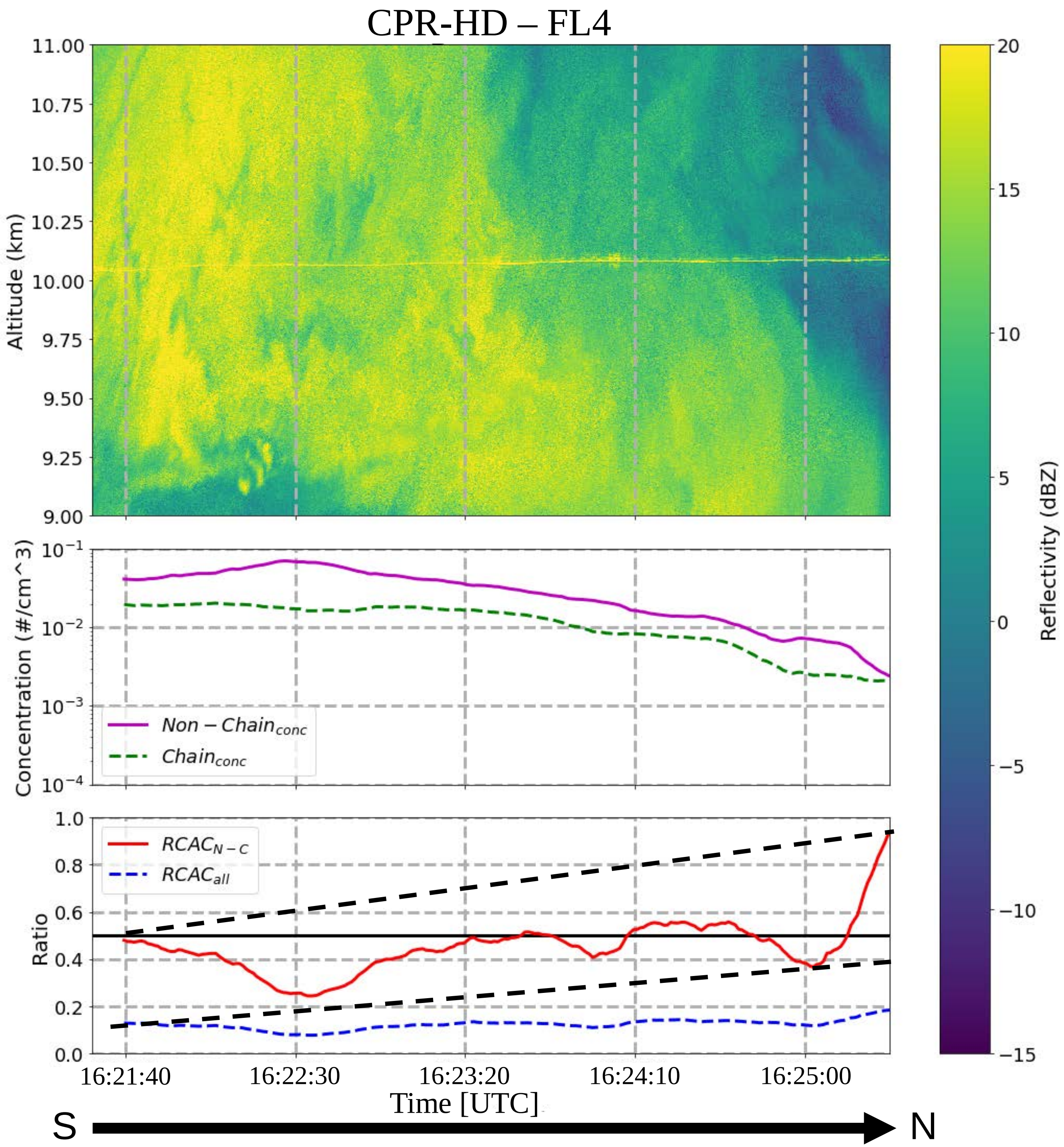

Future Work

- Further analysis on the other research flights during CapeEx19

- Future Campaigns:
  - Adjust Sampling Methods
  - Sample cirrus cloud anvils in other geographical regions.

- Perform more Cloud Chamber Experiments
  - Test if chain aggregation can occur using electric fields < 60 kV m^{-1} at temperatures less than -30 °C.

Acknowledgements

- Thesis Committee
- Naval Research Laboratory (NRL)
  - Mentor: Jerry Schmidt
- Special Thanks:
  - Josh Hoover, NSWC
  - Andy Detwiler, UND
  - Hugh Christian, UAH
  - Jeff Stith, NCAR
  - Ron Holle, Vaisala
  - Nick Gapp, UND/SAIC
  - Jake Mulholland, UND
  - Friends
  - Family

References

- Abdelmonem, A., E. Järvinen, D. Duft, E. Hirst, S. Vogt, T. Leisner, and M. Schnaiter, 2016: PHIPS–HALO: the airborne Particle Habit Imaging and Polar Scattering probe – Part 1: Design and operation. *Atmos. Meas. Tech.*, **9**, 3131–3144, https://doi.org/10.5194/amt-9-3131-2016.
- Barnes Jr., A. A., 1982: The Sub-visible Cirrus Background. Air Force Geophysics Laboratory. Date Accessed: 04-15-2021. https://apps.dtic.mil/dtic/tr/fulltext/u2/a117389.pdf.
- Bateman, M. G., M. F. Stewart, S. J. Podgorny, H. J. Christian, D. M. Mach, R. J. Blakeslee, J. C. Bailey, and D. Daskar, 2007: A Low-Noise, Microprocessor-Controlled, Internally Digitizing Rotating-Vane Electric Field Mill for Airborne Platforms. *J. Atmos. Oceanic Technol.*, **24**, 1245–1255, https://doi.org/10.1175/JTECH2039.1.
- Baumgardner, D., H. Jonsson, W. Dawson, D. O'Connor, and R. Newton, 2001: The cloud, aerosol and precipitation spectrometer: a new instrument for cloud investigations. *Atmospheric Research*, **59–60**, 251–264, https://doi.org/10.1016/S0169-8095(01)00119-3.
- Connolly, P. J., C. P. R. Saunders, M. W. Gallagher, K. N. Bower, M. J. Flynn, T. W. Choularton, J. Whiteway, and R. P. Lawson, 2005: Aircraft Observations of the Influence of Electric Fields on the Aggregation of Ice Crystals. *Quarterly Journal of the Royal Meteorological Society*, **131**, 1695–1712, https://doi.org/10.1256/qj.03.217.
- Crowther, A. G. and C. P. R. Saunders, 1973: On the Aggregation and Fragmentation of Freely-Falling Ice Crystals in an Electric Field. *J. Met. Soc. Japan*, **51**, 490-493.
- Dye, J. E., and A. Bansemer, 2019: Electrification in Mesoscale Updrafts of Deep Stratiform and Anvil Clouds in Florida. *Journal of Geophysical Research: Atmospheres*, **124**, 1021–1049, https://doi.org/10.1029/2018JD029130.
- Dye, J. E., and Coauthors, 2007: Electric fields, cloud microphysics, and reflectivity in anvils of Florida thunderstorms. *Journal of Geophysical Research: Atmospheres*, 112, https://doi.org/10.1029/2006JD007550.
- Dye, J. E., and J. C. Willett, 2007: Observed Enhancement of Reflectivity and the Electric Field in Long-Lived Florida Anvils. *Monthly Weather Review*, **135**, 3362–3380, https://doi.org/10.1175/MWR3484.1.
- Gapp, N. J., 2019: Comparison of Concurrent Radar and Aircraft Measurements in Cirrus Clouds. M.S. thesis, Dept. of Atmospheric Sciences, University of North Dakota, 54 pp.
- Garrett, T. J., and Coauthors, 2005: Evolution of a Florida Cirrus Anvil. *Journal of the Atmospheric Sciences*, **62**, 2352–2372, https://doi.org/10.1175/JAS3495.1.
- Gayet, J.-F., and Coauthors, 2012: On the observation of unusual high concentration of small chain-like aggregate ice crystals and large ice water contents near the top of a deep convective cloud during the CIRCLE-2 experiment. *Atmospheric Chemistry and Physics*, **12**, 727–744, https://doi.org/10.5194/acp-12-727-2012.
- Jensen, E., D. Starr, and O. B. Toon, 2004: Mission investigates tropical cirrus clouds. Eos, *Transactions American Geophysical Union*, **85**, 45–50, https://doi.org/10.1029/2004EO050002.

References

- Latham, J., 1969: Experimental studies of the effect of electric fields on the growth of cloud particles. *Quarterly Journal of the Royal Meteorological Society*, **95**, 349– 361, https://doi.org/10.1002/qj.49709540408.
- Latham, J., and C. P.R. Saunders, 1964: Aggregation of Ice Crystals in Strong Electric Fields, *Nature*, **204**, 1293 – 1294.
- Latham, J., and C. P. R. Saunders, 1970: Experimental measurements of the collection efficiencies of ice crystals in electric fields. *Quarterly Journal of the Royal Meteorological Society*, **96**, 257–265, https://doi.org/10.1002/qj.49709640808.
- Lawson, R. P., B. A. Baker, and B. L. Pilson, 2003: In Situ Measurements of Microphysical Properties of Mid-latitude and Anvil Cirrus. Date Accessed: 04-25-2021. http://www.specinc.com/sites/default/files/pdfs/Cirrus_Anvil_paper_Rev2_.pdf
- Lin, T. C., and N. A. Thyson, 1977: Ice-crystal/shock-layer interaction in hypersonic flight. *AIAA Journal*, **15**, 1511–1514, https://doi.org/10.2514/3.7446.
- Liou, K. N., 1973: Transfer of Solar Irradiance through Cirrus Cloud Layers., *J. Geophys. Res.*, **78**, 1409–1418.
- Meng, H.C. and K.C. Ludema, 1995: Wear models and predictive equations: their form and content, *WEAR*, **181-183**, 443-457.
- NCAR, 2021a: MDV Format Interface Control Document (ICD). Accessed 10 June 2020, https://www.github.com/NCAR/lrose-titan/blob/master/docsa/pdf/MDV_format_ICD.pdf.
- NCAR, 2021b: TITAN. Accessed 10 June 2020, https://www.github.com/NCAR/lrose-titan.
- O'Shea, S. J., J. Crosier, J. Dorsey, W. Schledewitz, I. Crawford, S. Borrmann, R. Cotton, and A. Bansemer, 2019: Revisiting particle sizing using grayscale optical array probes evaluation using laboratory experiments and synthetic data. *Atmos. Meas. Tech. Discuss.*, 1–29, https://doi.org/10.5194/amt-2018-435.
- Probstein, R. F.; Fassio, F. Dusty Hypersonic Flows. *AIAA J.* **1970**, *8* (4), 772–779. https://doi.org/10.2514/3.5755.
- Rakov, V. A., 2016, General picture, *Fundamentals of Lightning*, Cambridge University Press, 52-65.
- Saunders, C. P. R., and N. M. A. Wahab, 1975: The Influence of Electric Fields on the Aggregation of Ice Crystals. *Journal of the Meteorological Society of Japan*, **53**, 121–126, https://doi.org/10.2151/jmsj1965.53.2_121

References

- Schmidt, J. M., and Coauthors, 2019: Radar Detection of Individual Raindrops. *Bulletin of the American Meteorological Society*, **100**, 2433–2450, https://doi.org/10.1175/BAMS-D-18-0130.1.
- Schnaiter, M., E. Järvinen, A. Abdelmonem, and T. Leisner, 2018: PHIPS-HALO: the airborne particle habit imaging and polar scattering probe – Part 2: Characterization and first results. *Atmos. Meas. Tech.*, **11**, 341–357, https://doi.org/10.5194/amt-11-341-2018.
- Smith, P. L., D. J. Musil, A. G. Detwiler, and R. Ramachandran, 1999: Observations of Mixed-Phase Precipitation within a CaPE Thunderstorm. *Journal of Applied Meteorology and Climatology*, **38**, 145–155, https://doi.org/10.1175/1520-0450(1999)038<0145:OOMPPW>2.0.CO;2.
- Stith, J. L., J. E. Dye, A. Bansemer, A. J. Heymsfield, C. A. Grainger, W. A. Petersen, and R. Cifelli, 2002: Microphysical Observations of Tropical Clouds. *J. Appl. Meteor.*, **41**, 97–117, https://doi.org/10.1175/1520-0450(2002)041<0097:MOOTC>2.0.CO;2.
- Stith, J. L., J. A. Haggerty, A. Heymsfield, and C. A. Grainger, 2004: Microphysical Characteristics of Tropical Updrafts in Clean Conditions. *Journal of Applied Meteorology and Climatology*, **43**, 779–794, https://doi.org/10.1175/2104.1.
- Stith, J. L., and Coauthors, 2014: Ice particles in the upper anvil regions of midlatitude continental thunderstorms: the case for frozen-drop aggregates. *Atmos. Chem. Phys.*, **14**, 1973–1985, https://doi.org/10.5194/acp-14-1973-2014.
- Um, J., and Coauthors, 2018: Microphysical characteristics of frozen droplet aggregates from deep convective clouds. *Atmospheric Chemistry and Physics*, **18**, 16915–16930, https://doi.org/10.5194/acp-18-16915-2018.
- Waldman, G. D.; Reinecke, W. G. Particle Trajectories, Heating, and Breakup in Hypersonic Shock Layers. *AIAA J.* **1971**, *9* (6), 1040–1048. https://doi.org/10.2514/3.6328.
- Whiteway, J., and Coauthors, 2004: Anatomy of cirrus clouds: Results from the Emerald airborne campaigns. *Geophysical Research Letters*, **31**, https://doi.org/10.1029/2004GL021201.

Questions?

EXTRA SLIDES

Flight Legs (FL)

- Four total FL defined on the 3 August 2019 research flight.

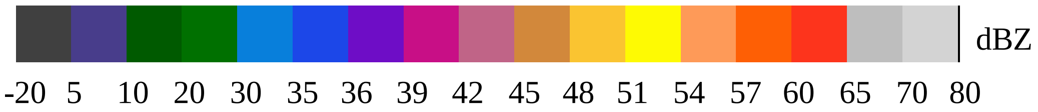

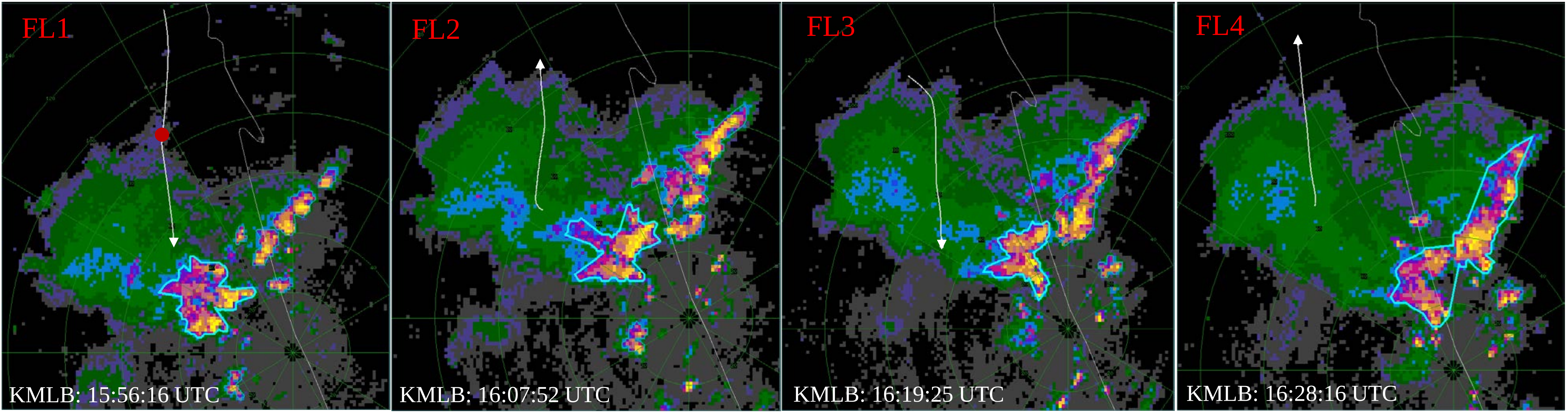

Legs	Time Span (hh:mm:ss)	Heading	Altitude	Temperature
FL1	15:51:15-16:01:00 UTC	Southbound	10,029 (± 4) m	-33.7 (± 0.4) °C
FL2	16:02:00-16:07:00 UTC	Northbound	10,034 (± 5) m	-33.4 (± 0.3) °C
FL3	16:09:00-16:17:00 UTC	Southbound	10,035 (± 5) m	-32.6 (± 0.9) °C
FL4	16:21:30-16:26:55 UTC	Northbound	10,021 (± 7) m	-29.8 (± 0.3) °C

Electric Field Reference Coordinates

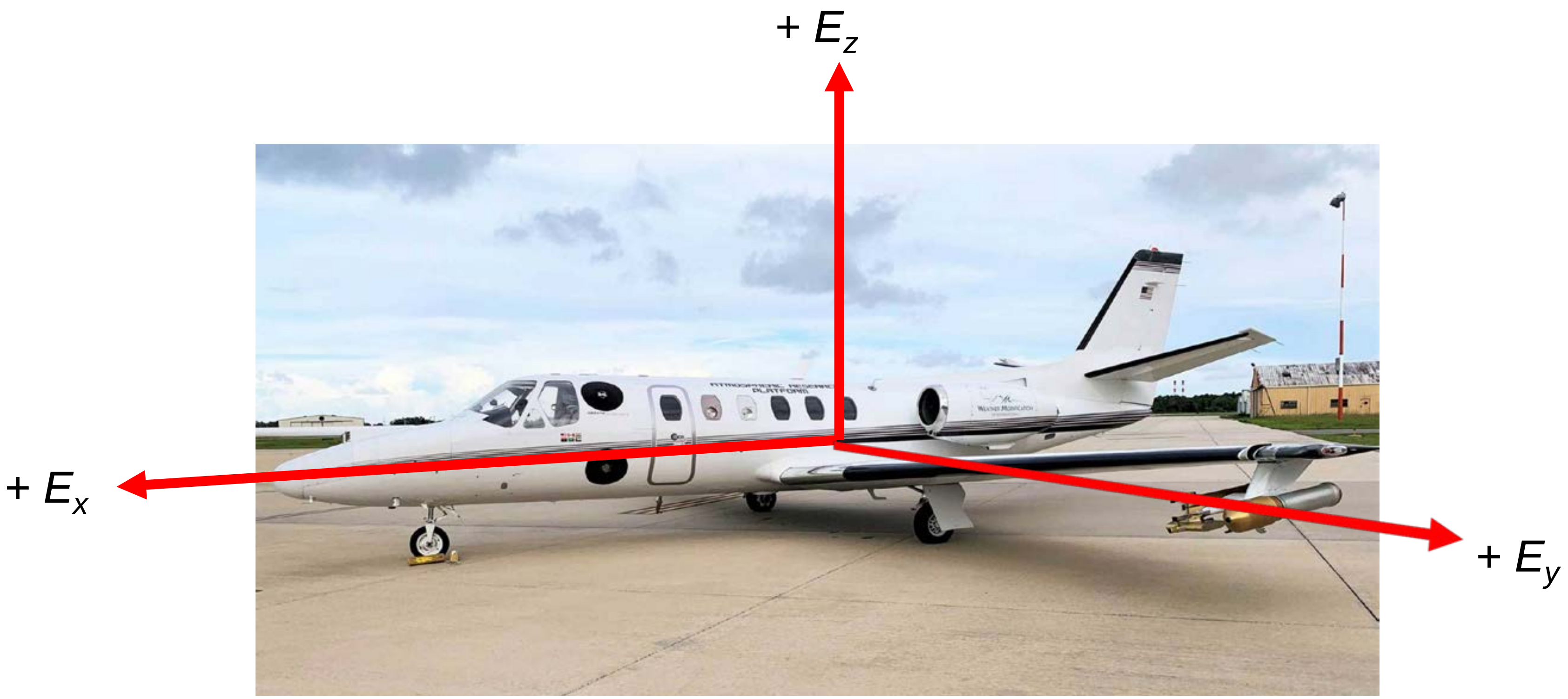

	70 – 100 km from Storm Core		40 – 70 km from Storm Core		10 – 40 km from Storm Core	
Legs	# of Images	All Confidences	# of Images	All Confidences	# of Images	All Confidences
FL1	510	11.4 ± 1.0% (N=58)	631	19.7 ± 1.0% (N=124)	366	9.8 ± 1.1% (N=36)
FL2	N/A	N/A	520	15.0 ± 1.0% (N=78)	397	10.1 ± 1.1% (N=40)
FL3	55	32.7 ± 3.3% (N=18)	800	15.1 ± 0.8% (N=121)	520	10.0 ± 1.0% (N=52)
FL4	178	24.7 ± 1.9% (N=44)	677	14.3 ± 0.9% (N=97)	N/A	N/A
TOTAL	743	16.2 ± 0.9% (N=120)	2,628	16.0 ± 0.5% (N=420)	1,283	10.0 ± 0.6% (N=128)

LMA Observations

LMA – 15:50:00 – 16:00:00 UTC

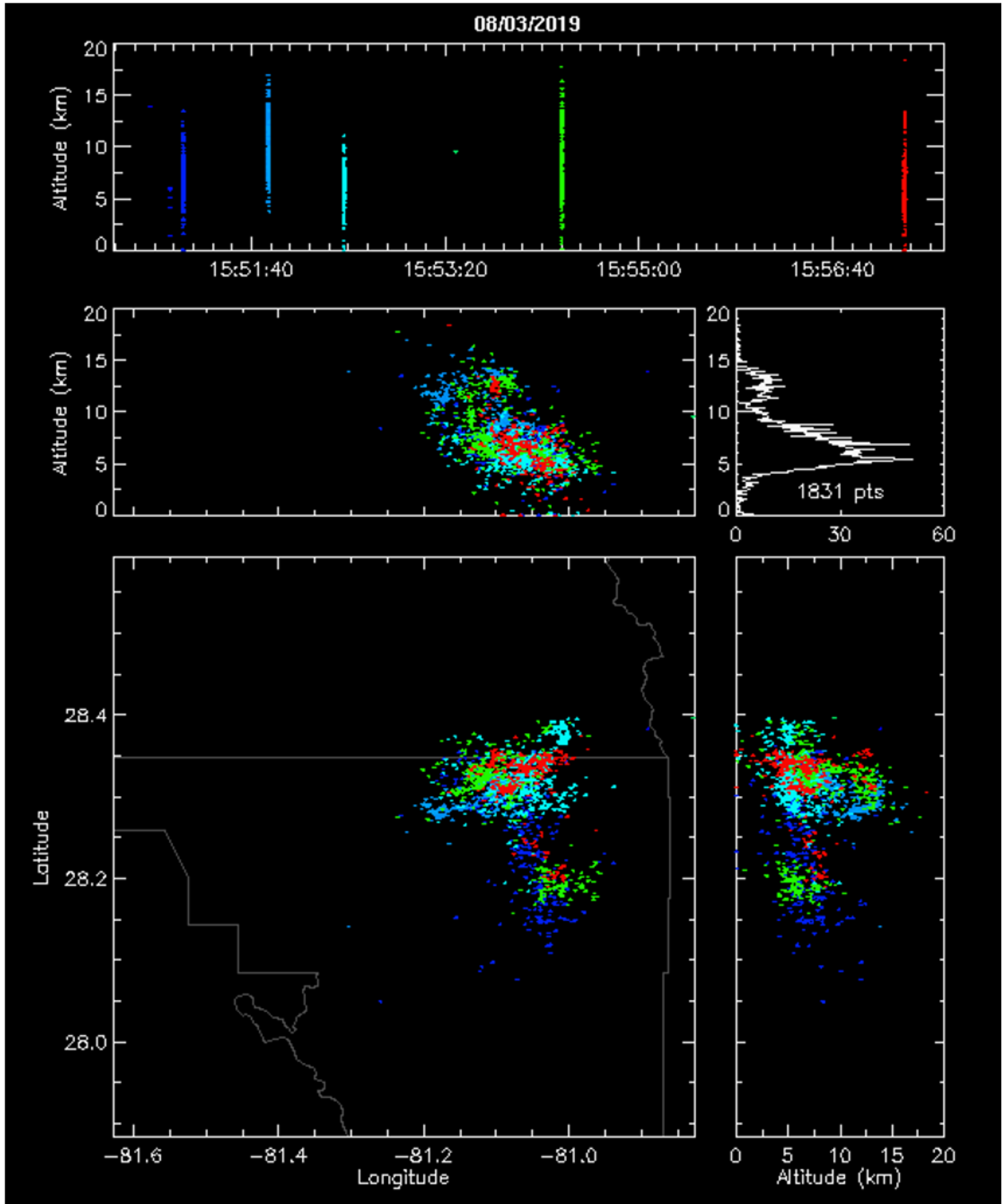

LMA Observations

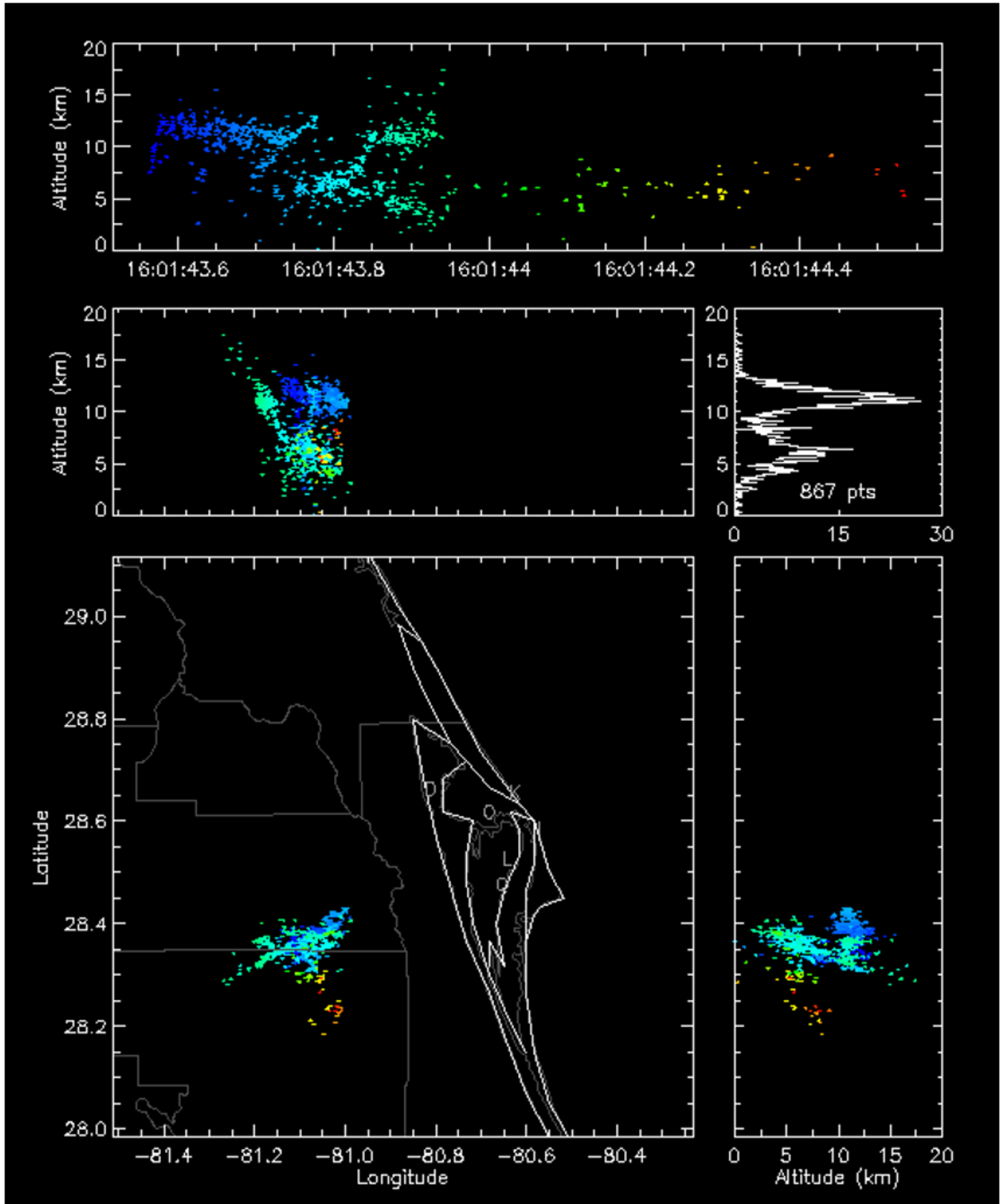

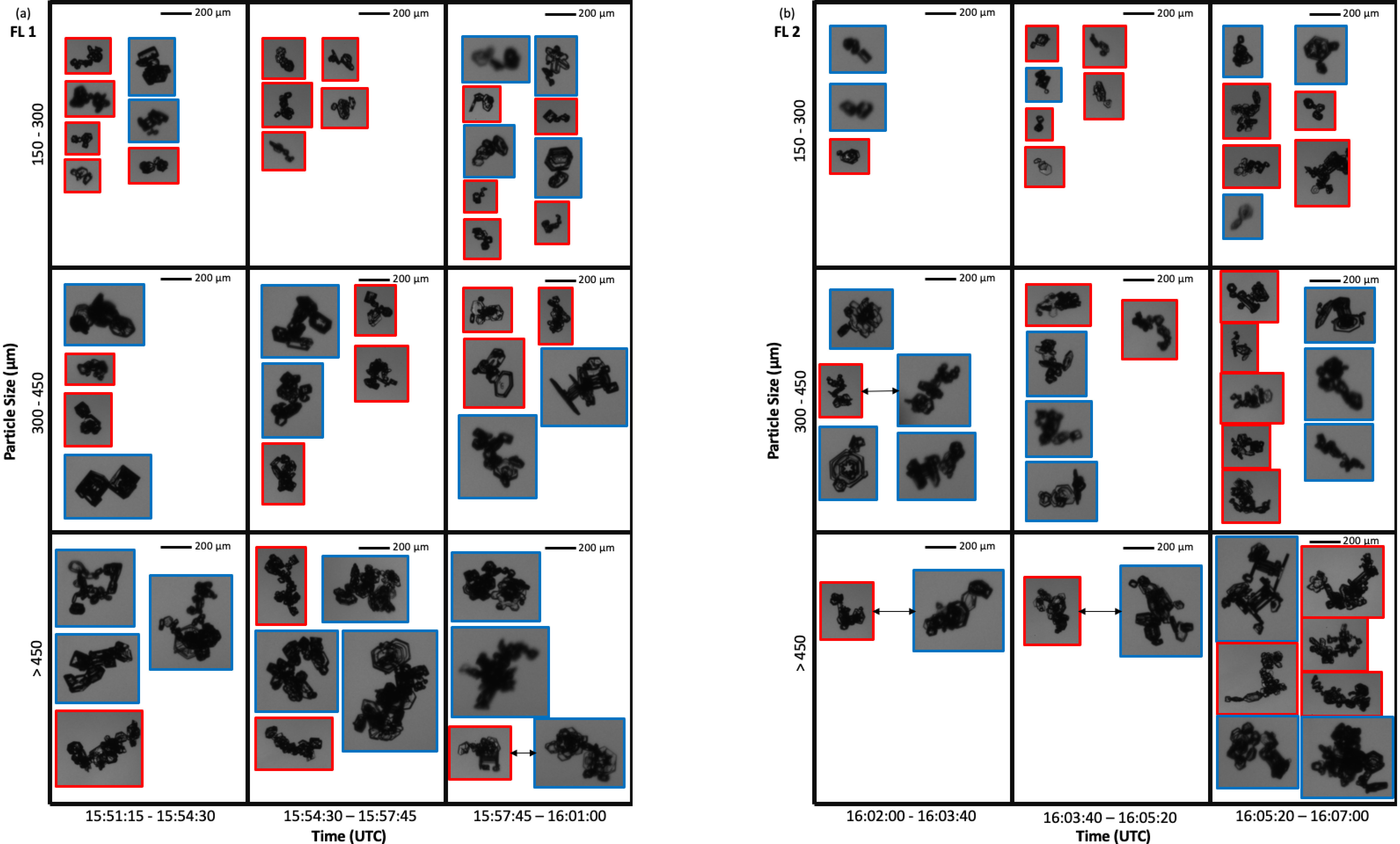
(a)
FL 1
(b)
FL 2
200 µm
Particle Size (µm)
150 - 300
300 - 450
> 450
15:51:15 - 15:54:30
15:54:30 – 15:57:45
15:57:45 – 16:01:00
16:02:00 - 16:03:40
16:03:40 – 16:05:20
16:05:20 – 16:07:00
Time (UTC)

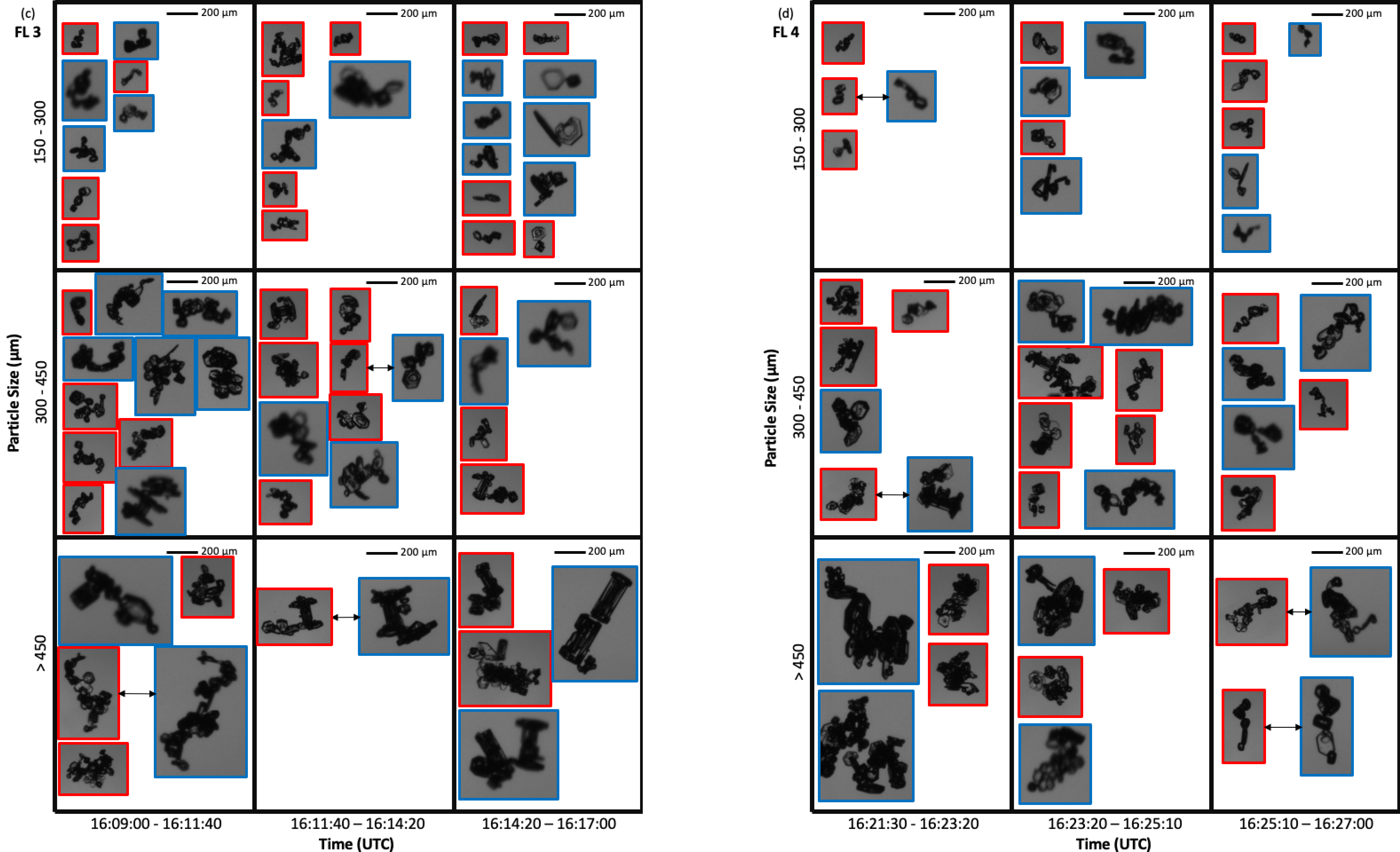
(c)
FL 3
150 - 300
300 - 450
> 450
Particle Size (µm)
200 µm
16:09:00 - 16:11:40
16:11:40 – 16:14:20
16:14:20 – 16:17:00
Time (UTC)
(d)
FL 4
150 - 300
300 - 450
> 450
Particle Size (µm)
200 µm
16:21:30 - 16:23:20
16:23:20 – 16:25:10
16:25:10 – 16:27:00
Time (UTC)

Rimed Chain Example

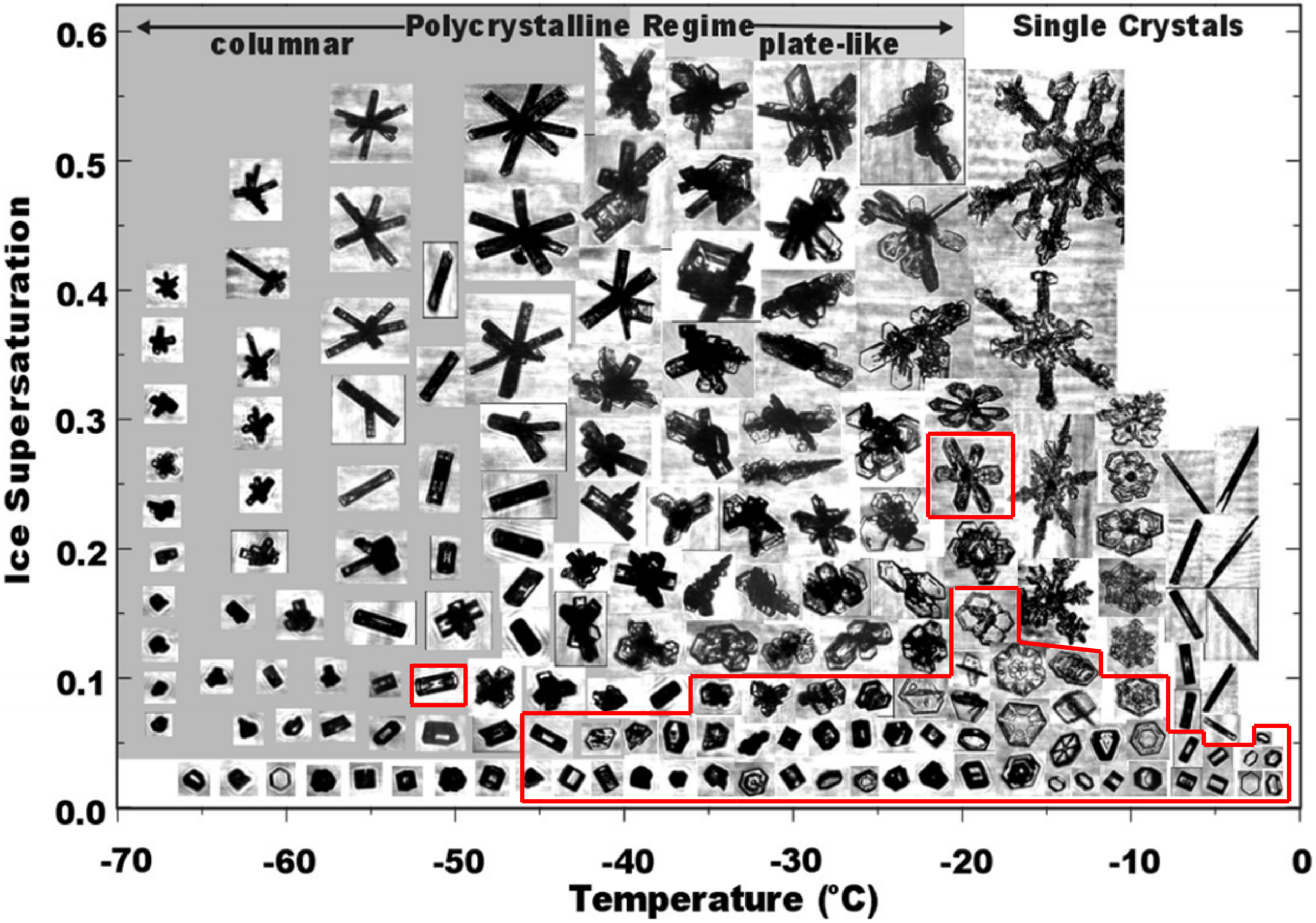
Polycrystalline Regime
columnar
plate-like
Single Crystals
Ice Supersaturation
0.6
0.5
0.4
0.3
0.2
0.1
0.0
-70
-60
-50
-40
-30
-20
-10
0
Temperature (°C)

15:00 UTC Sounding from Cape Canaveral, Florida

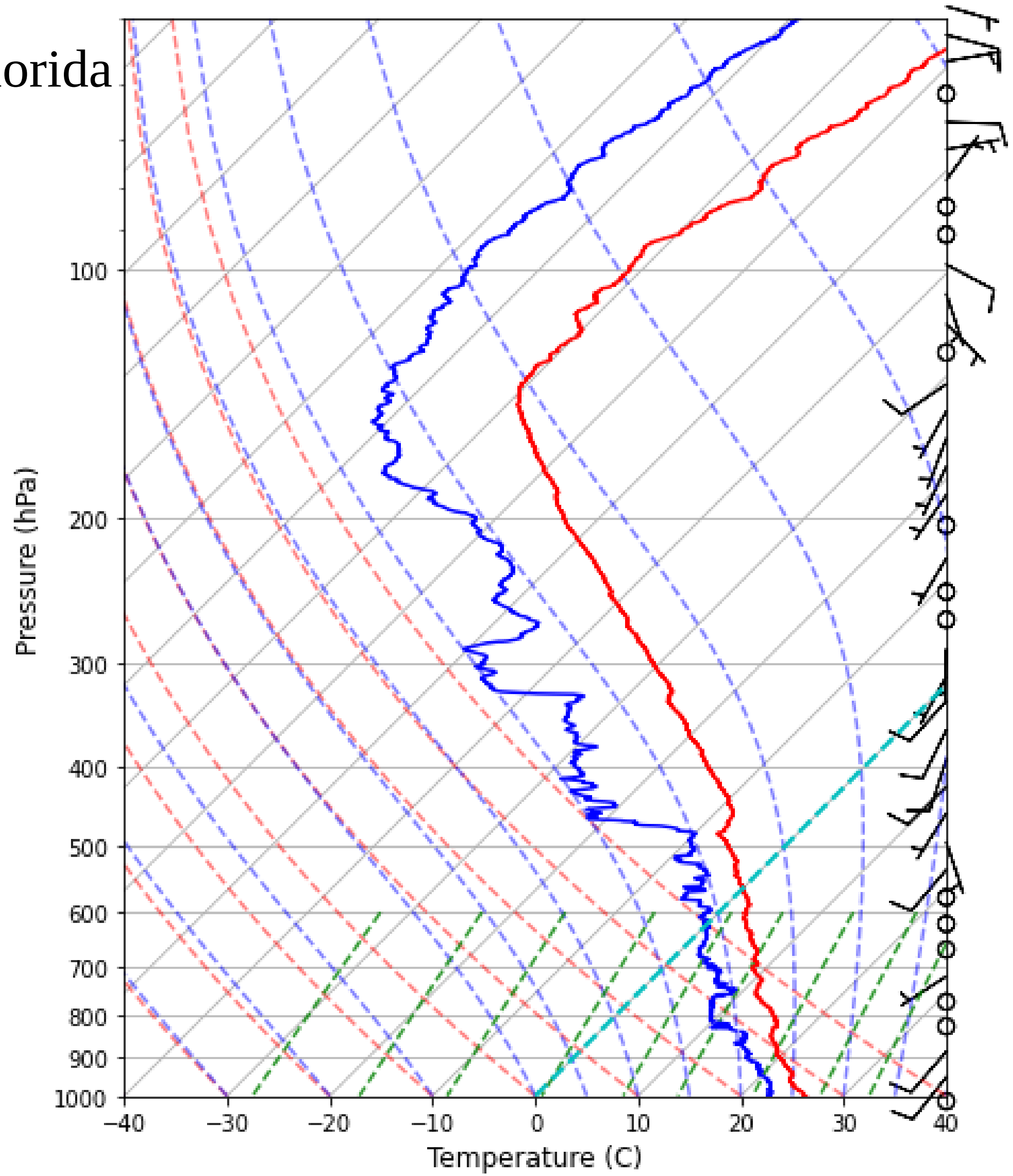

Flight Leg 1 (FL1)

15:51:15 – 16:01:00

KMLB Vol Scan: 15:50:30

10 km CAPPI

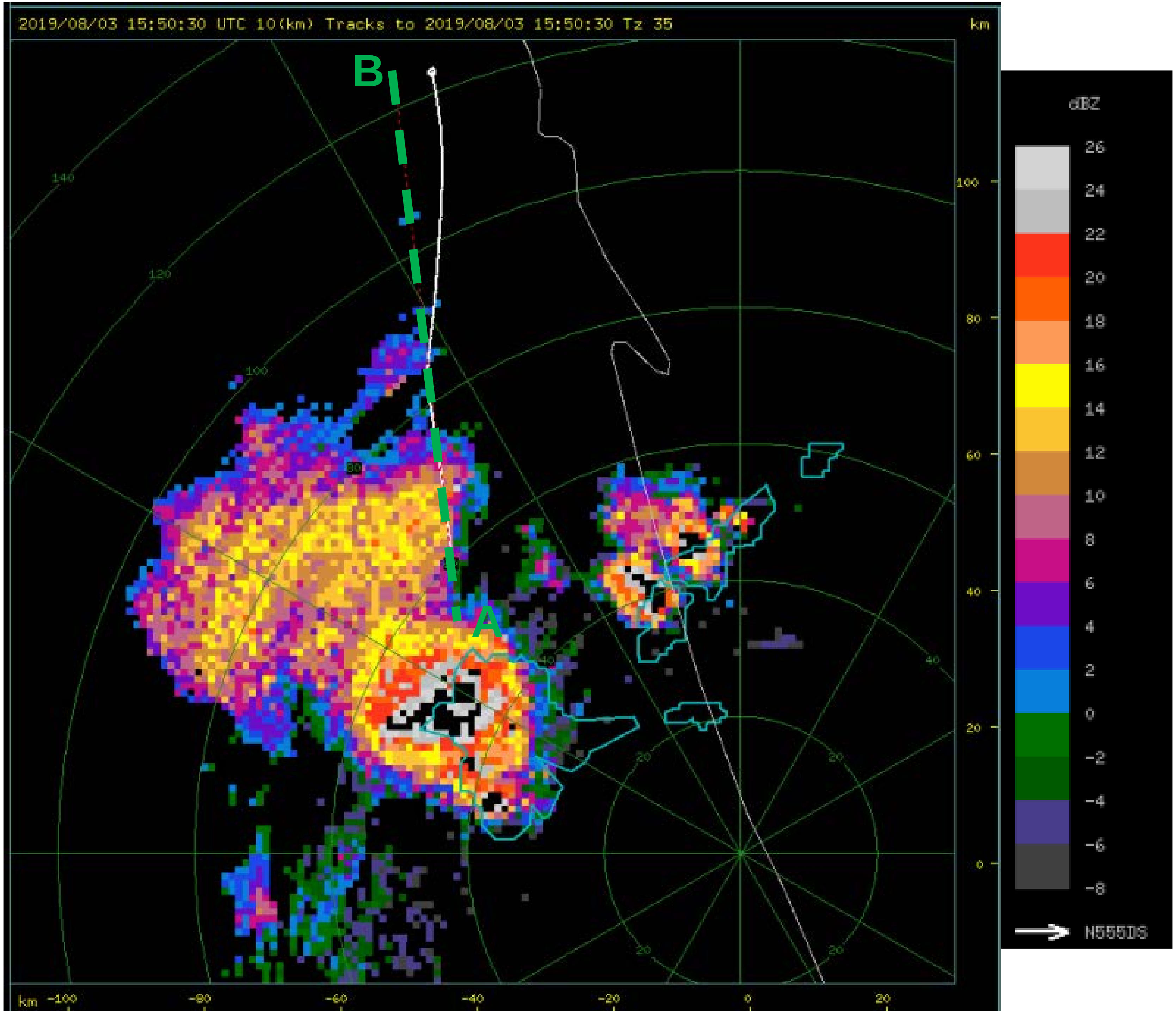

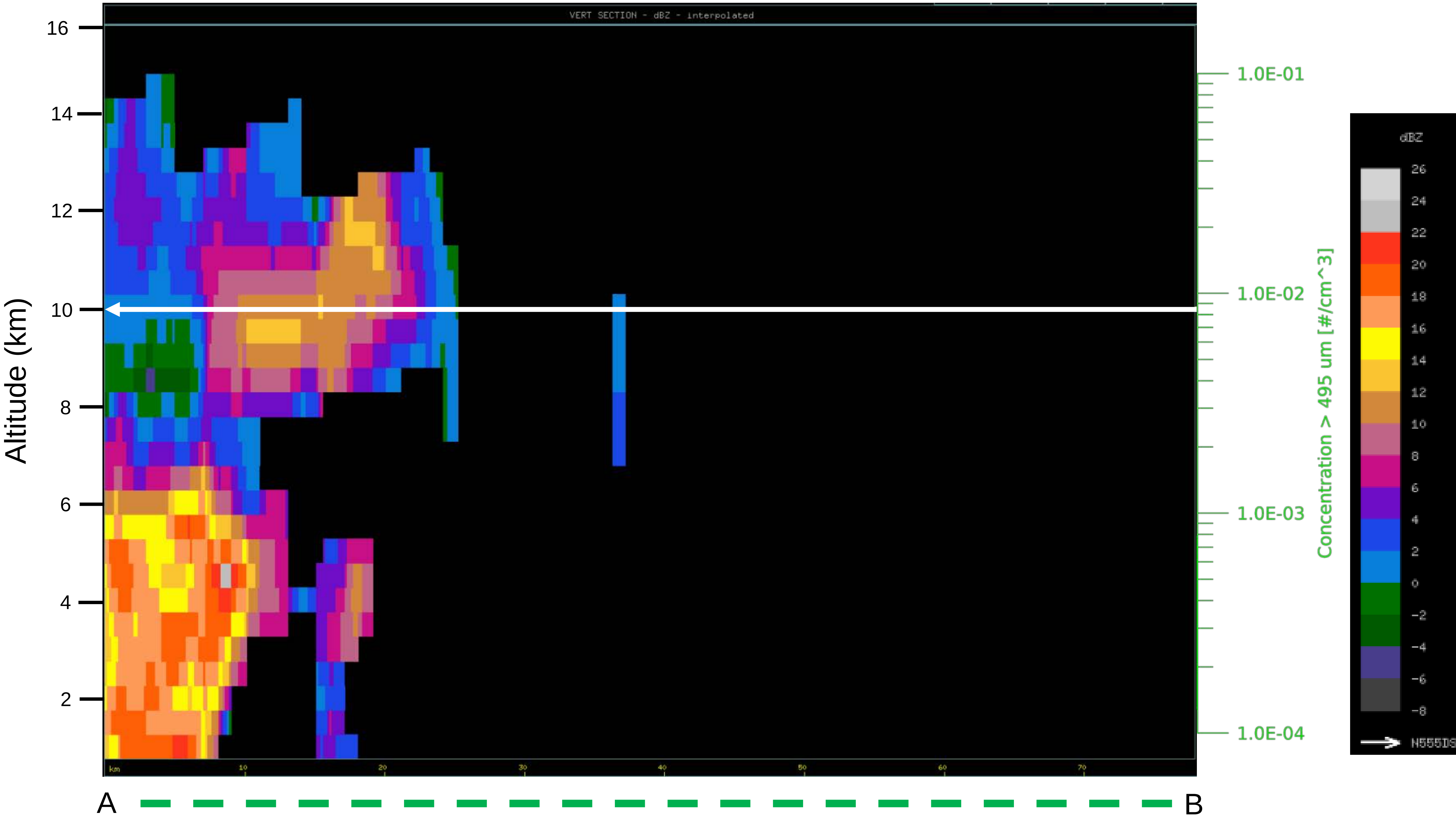
VERT SECTION - dBZ - interpolated
Altitude (km)
16
14
12
10
8
6
4
2
km
10
20
30
40
50
60
70
1.0E-01
1.0E-02
1.0E-03
1.0E-04
Concentration > 495 um [#/cm^3]
dBZ
26
24
22
20
18
16
14
12
10
8
6
4
2
0
-2
-4
-6
-8
A
B

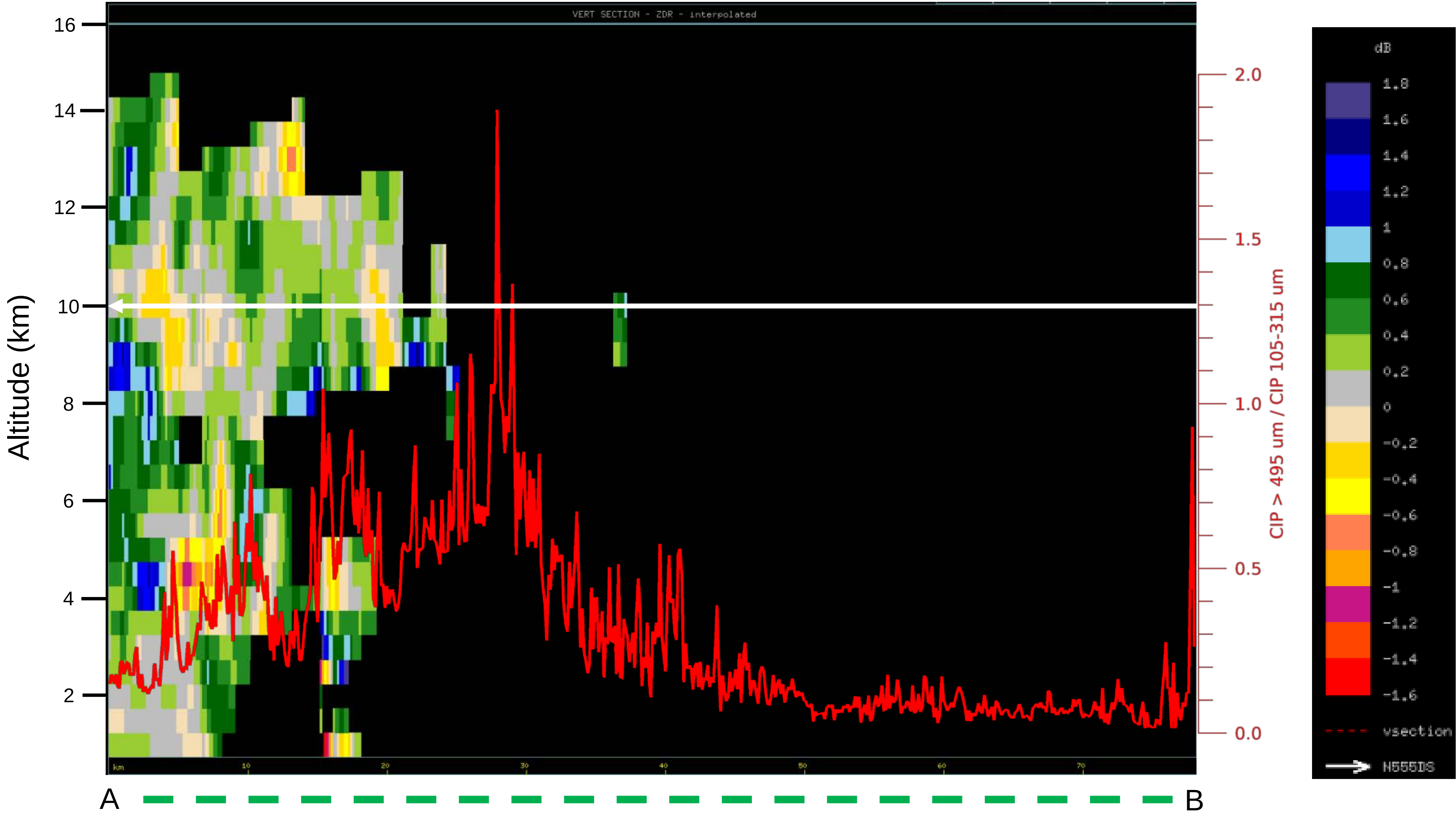

VERT SECTION - ZDR - interpolated
Altitude (km)
16
14
12
10
8
6
4
2
CIP > 495 um / CIP 105-315 um
2.0
1.5
1.0
0.5
0.0
km
10
20
30
40
50
60
70
A
B
dB
1.8
1.6
1.4
1.2
1
0.8
0.6
0.4
0.2
0
-0.2
-0.4
-0.6
-0.8
-1
-1.2
-1.4
-1.6
vsection
N555DS

Uncertainty Analysis (PHIPS chains) – Baird 1994

Product of Two or More Variables (SEC 2-9)

a.) $z = \frac{Chains}{Total\ \#\ Particles} = \frac{x}{y} = xy^{-1}$; x^a, y^b ; $\delta x = \sqrt{x}, \delta y = \sqrt{y}$

b.) $\log(z) = a * \log(x) + b * \log(y)$

c.) $\log(z) = a * \log(x) - b * \log(y)$

d.) $\frac{\delta z}{z} = a\frac{\delta x}{x} - b\frac{\delta y}{y}$

e.) $\delta z = z(a\frac{\delta x}{x} - b\frac{\delta y}{y})$

PHIPS Classification Software